PROCEEDINGS, 48th Workshop on Geothermal Reservoir Engineering
Stanford University, Stanford, California, February 6-8, 2023
SGP-TR-224

Enablement of High-Temperature Well Drilling for Multilateral Closed-Loop Geothermal Systems

Colin A. Brown, Michael Holmes, Vlad Zatonski, Matt Toews

Eavor Technologies Inc., Calgary, Alberta

Colin.Brown@eavor.com, Mike.Holmes@eavor.com, Vlad.Zatonski@eavor.com, Matt.Toews@eavor.com

Keywords: Geothermal, closed-loop geothermal, advanced geothermal systems, Eavor-Loop, Eavor-Deep, high pressure high temperature, thermodynamics, renewable, green energy, insulated drill pipe

ABSTRACT

Constructing a multilateral closed-loop geothermal system (MCLGS) requires directional tools and magnetic ranging tools in the bottom-hole assembly (BHA) to drill and intersect the wellbores and create the closed loop. The levelized cost of energy (LCOE) of such an MCLGS is largely driven by rock temperature – the hotter the rock, the more energy that is produced from a given well configuration, and the lower the levelized cost. However, these tools have a maximum temperature limit above which they are no longer functional. To enable drilling of high-temperature rock formations and thereby decrease the LCOE, methods for estimating the temperature of the BHA critical components are required.

To simulate drilling, two models of increasing complexity were developed. The first model is a one-dimensional pseudo steady state wellbore + thermal resistance model capable of estimating the temperature and pressure profile of the drilling mud throughout the drill pipe and annulus. This model allows for the understanding of key performance drivers and technology requirements to achieve high-temperature drilling.

The second model is a transient, two-dimensional heat conduction and wellbore model. This coupled model enables simulation of the fluid temperature and pressure during dynamic drilling processes such as connections, running in hole, pulling out of hole, and circulation.

This paper illustrates the capabilities of the two models and presents case studies and key learnings for high-temperature drilling as well as field results from Eavor's deep hot test well drilled in Q4 2022 in New Mexico, USA.

1. INTRODUCTION

1.1 Eavor-Loop™: a Multilateral Closed-Loop Geothermal System

Multilateral closed-loop geothermal systems (MCLGS), a form of Advanced Geothermal System (AGS), are geothermal systems in which a heat transfer fluid – e.g. water – circulates in a closed-loop configuration. Unlike a traditional geothermal system, there is little-to-no mass transfer between the MCLGS wellbore and the subsurface. The circulating fluid picks up heat from the subsurface via heat conduction and transports the heat to the surface which can be used for district heat (common in Europe) or converted into electricity (e.g. through an Organic Rankine Cycle power plant). MCLGS and other AGS technologies compared to other forms of geothermal systems are theoretically capable of being developed anywhere without the need for in-situ fluids and reservoir permeability – expanding the applicability of geothermal energy across the globe.

Eavor's Eavor-Loop™ technology is a form of MCLGS (and AGS). Over the years, various studies have been completed evaluating the techno-economic applicability of AGS systems, e.g. Beckers et al (2022). In all such studies, economic viability of an Eavor-Loop™ and other AGS technologies require significant heat transfer surface area, which require complex subsurface completions and high reservoir temperatures.

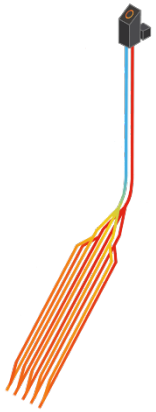

Figure 1: Illustration of an Eavor-Loop™

Due to the relatively slow rate of heat transfer via conduction through the subsurface rock, several dozens of kilometers of wellbore need to be drilled and connected to achieve an economic amount of heat transfer surface area. To achieve the complex subsurface layout of the Eavor-Loop™, directional drilling and magnetic ranging tools in the bottom-hole assembly (BHA) are required to drill and intersect the multiple lateral passes. However, the temperature limits of current ranging tools pose a technical challenge. The current generation of these tools are rated to temperatures in the range of 150-175 °C, while rock temperatures could reach up to 450 °C. To successfully drill and complete an Eavor-Loop™, the bottom-hole-assembly (BHA) components either need to be re-engineered for higher temperatures or need to be kept cool during drilling operations.

1.2 Enabling High Pressure, High Temperature (HPHT) Drilling

Creating tools that are tolerant of higher temperatures would require the re-engineering of key components and may require large amounts of R&D spend. Solutions that keep the tools cool while drilling are simpler, and depending on the solution, are cheaper than completely re-engineering the tools and/or its components. For example, improving the thermal resistance of the drill pipe will reduce the counter-current heat exchange between the annular fluid and tubular fluid, thereby reducing the bottom-hole fluid temperatures.

A drill pipe with improved thermal resistance was used to drill Eavor's hot pilot well, Eavor-Deep™, in New Mexico, USA with promising results. Drilling operations were safely completed in Q4 of 2022.

1.3 Modelling

Regardless of the approach to enable HPHT drilling, thermodynamic modelling is critical to evaluate the feasibility of drilling and completion of HPHT Eavor-Loops™, as well as the evaluation of different "cooling" technologies.

Two thermodynamic models were developed, each of differing complexity, to determine the pressures and temperatures within the wellbore while drilling. The first model is a one-dimensional pseudo steady-state wellbore model capable of estimating the annular and tubular pressures and temperatures (referred to as the "steady-state" model). This model is limited to estimating steady-state fluid pressures and temperatures. The second model is a transient two-dimensional heat conduction and wellbore model (referred to as the "transient" model). Like the steady-state model, the transient model simulates the annular and tubular fluid pressures and temperatures, but the transient model also reports the pressures and temperatures during transient drilling operations where the drill pipe, circulation rate, and mud characteristics are changing with time.

The difference in the high-level characteristics of the two models are summarized in the table below.

Table 1: Model characteristics summary

Model Characteristic	Steady-State Model	Transient Model
Wellbore equations, momentum	Steady-state	Steady-state
Wellbore equations, energy	Steady-state	Transient
Rock equations	Pseudo-transient	Transient
Application / Language	Microsoft Excel	Python
Run time, order of magnitude	Seconds	Minute to 10's of minutes (depends on number of time-steps)

2. PSEUDO STEADY-STATE MODEL

2.1 Model Formulation

The steady-state model is a pseudo steady-state, 1-D, discretized wellbore drilling model. A schematic of the steady-state model setup is shown in Figure 2 below.

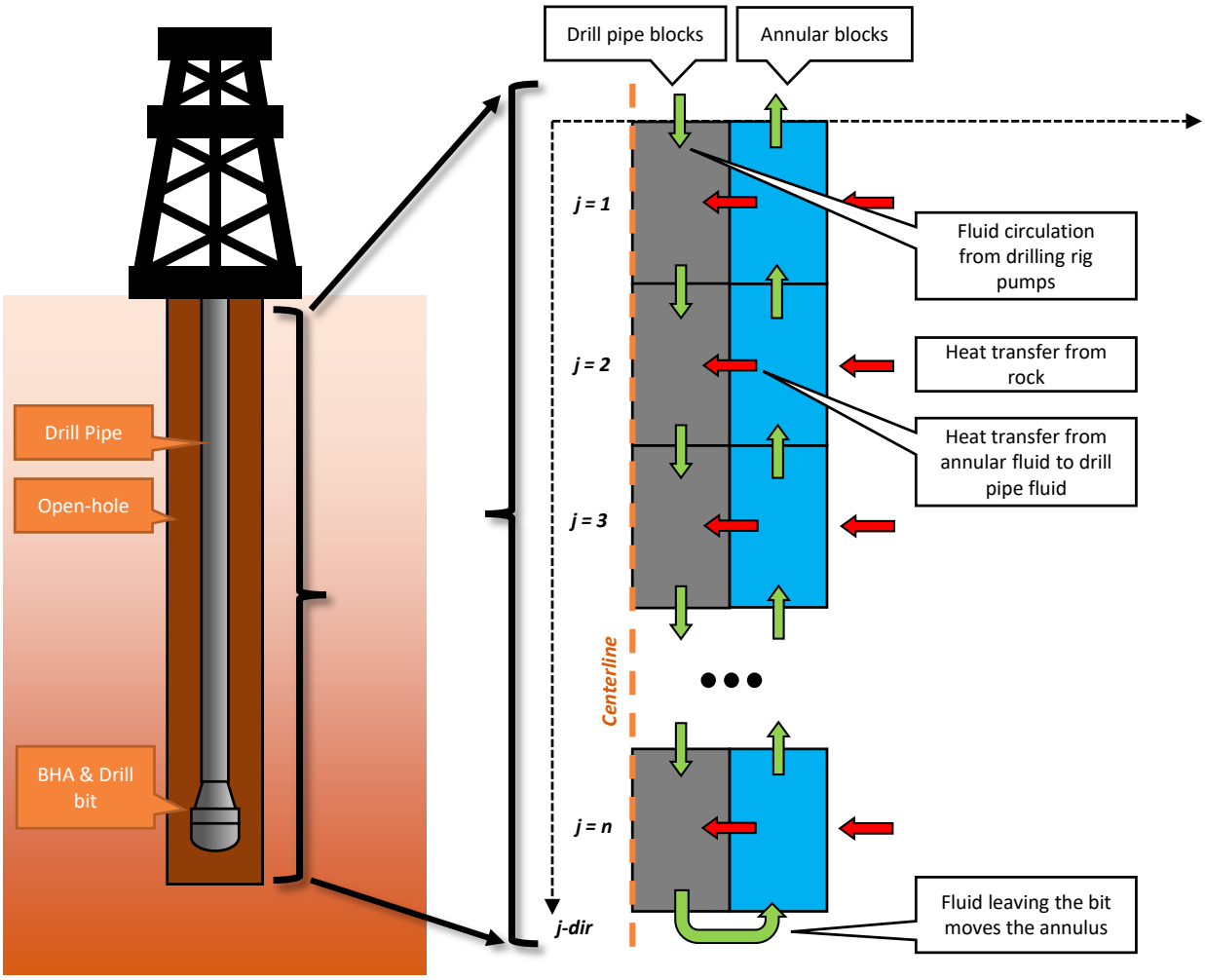

Figure 2: Steady-state model schematic. Green arrows indicate mass transfer (flow) while red arrows indicate heat transfer.

The wellbore system is naturally divided into two fluid-bearing sections: (1) the drill-pipe / tubing, and (2) the annular space between the drill-pipe and the open hole/rock face. The system is further discretized in the well direction (denoted as the j-direction in the schematic). Since the drill pipe blocks and annular blocks are considered together in the solution of this system, the model effectively only has one dimension – in the direction of the well.

2.2 Governing Equations and Assumptions

To simplify the resulting model, the following assumptions are made:

1. The change in kinetic energy is neglected in the conservation of energy equation since its contribution is small compared to the internal energy and enthalpy change of the fluid.

2. We are interested in the steady-state solution to the conservation of energy equations, i.e. we assume $\frac{\partial E}{\partial t} = 0$

3. The conservation of mass has been invoked for an incompressible fluid so the mass flux is constant along the length of the wellbore.

4. A simplified, pseudo-steady version of the momentum equation is employed whereby the pressure drop is directly related to the frictional pressure drop using the Colebrook White type correlation.

5. Neglect the impact of rock cuttings on the fluid properties (e.g. specific heat, density, viscosity), and the energy balance.

The governing conservation equations are derived for the individual control volumes that correspond to the drill pipe blocks and annulus blocks. Figure 3 illustrates the generalized control volumes for the drill pipe blocks and annulus blocks.

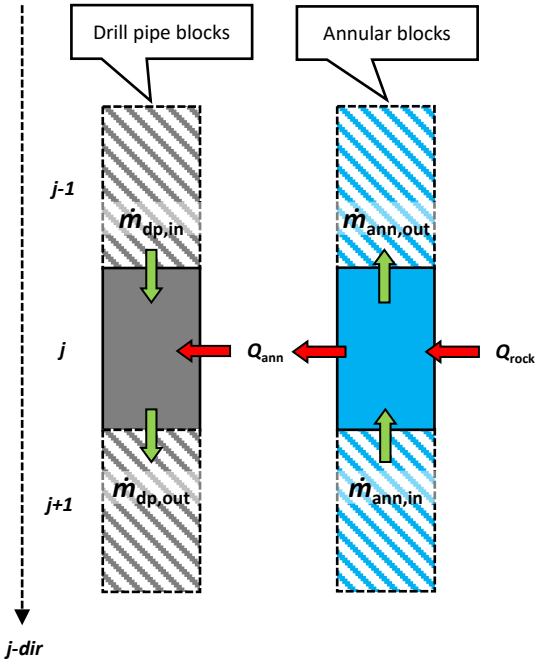

Figure 3: Steady-state model control volume schematics for the drill pipe and annulus blocks

Each of the colored arrows in Figure 3 represent the mass and energy flows within the wellbore system. For each j-section, direction of the mass and energy flows into and out of each of the blocks will be similar (although magnitudes will differ).

Since we have assumed a steady-state conservation of mass equation, there is no change in mass within each control volume. The mass flux into a block is equal to the mass flux out of a block. Therefore,

$$\dot{m} = \dot{m}_{\text{tbg,in}} = \dot{m}_{\text{tbg,out}} = \dot{m}_{\text{ann,in}} = \dot{m}_{\text{ann,out}} \quad (1)$$

The use of the simplified pseudo-steady momentum equation gives the following pressure drop equation for a generic drill pipe, and annulus block

Drill pipe:
$$p_{j-1} - p_j = \left(f_{\text{D}} \cdot L \cdot \frac{\rho_{j-1}}{2} \cdot \frac{{v_{j-1}}^2}{D_{\text{H}}}\right) - \left(\rho_{j-1} \cdot g \cdot \left(z_j - z_{j-1}\right)\right) \quad (2)$$

Annulus:
$$p_{j-1} - p_j = -\left(f_{\text{D}} \cdot L \cdot \frac{\rho_{j-1}}{2} \cdot \frac{{v_{j-1}}^2}{D_{\text{H}}}\right) - \left(\rho_{j-1} \cdot g \cdot \left(z_j - z_{j-1}\right)\right) \quad (3)$$

where p is the pressure in the grid block/control volume

f_{D} is the Darcy friction factor

L is the length of the grid block/control volume in the axial direction

ρ is the density of the drilling fluid

v is the velocity of the drilling fluid

D_{H} is the hydraulic diameter

g is the gravitational constant (i.e. 9.81 m/s^2)

z is the total vertical depth of the grid block/control volume

j is the grid block index in the direction of the well path

For a generic drill pipe block, the steady-state conservation of energy equation can be expressed to include the heat transfer terms implied by the arrows in Figure 3.

$$\dot{m}h_{\mathrm{dp},j-1} + \dot{Q}_{\mathrm{ann}} + \dot{m}g\left(z_j - z_{j-1}\right) = \dot{m}h_{\mathrm{dp},j} \quad (4)$$

where $\dot{m}$ is the mass flow rate/circulation rate of the drilling fluid

$h_{\mathrm{dp},j-1}$ is the enthalpy of the drilling fluid in the drill pipe segment at *j-1*

$h_{\mathrm{dp},j}$ is the enthalpy of the drilling fluid in the drill pipe segment at *j*

$\dot{Q}_{\mathrm{ann}}$ is the heat transfer rate from the annulus block to the drill pipe block

Similarly, the steady-state conservation of energy equation for a generic annulus block gives

$$\dot{m}h_{\mathrm{ann},j+1} + \dot{Q}_{\mathrm{rock}} = \dot{m}h_{\mathrm{ann},j} + \dot{Q}_{\mathrm{ann}} + \dot{m}g\left(z_j - z_{j-1}\right) \quad (5)$$

where $h_{\mathrm{ann},j+1}$ is the enthalpy of the drilling fluid in the annulus segment at *j+1*

$h_{\mathrm{ann},j}$ is the enthalpy of the drilling fluid in the annulus segment at *j*

$\dot{Q}_{\mathrm{rock}}$ is the heat transfer rate from the rock formation to the annulus block

The heat transfer rate between the annular fluid and the drill pipe fluid, $\dot{Q}_{\mathrm{ann}}$, is an expression that combines conductive and convective resistances:

$$\dot{Q}_{\mathrm{ann},j} = \frac{T_{\mathrm{ann},j} - T_{\mathrm{dp},j}}{R_{\mathrm{ann},j}} \quad (6)$$

$$R_{\mathrm{ann},j} = R_{\mathrm{conv,dp},j} + R_{\mathrm{cond,dp\ wall},j} + R_{\mathrm{conv,ann},j} \quad (7)$$

where $T_{\mathrm{dp},j}$ is the temperature of the fluid in the drill pipe

$T_{\mathrm{ann},j}$ is the temperature of the fluid in the annulus

$R_{\mathrm{ann},j}$ is the total thermal resistance between the drill pipe and annulus fluids

$R_{\mathrm{conv,dp},j}$ is the convective thermal resistance at the inside face of the drill pipe

$R_{\mathrm{cond,dp\ wall},j}$ is the conductive thermal resistance through the drill pipe wall

$R_{\mathrm{conv,ann},j}$ is the convective thermal resistance at the outside face of the drill pipe

Generally, convective thermal resistances are defined as follows:

$$R_{\mathrm{conv}} = \frac{1}{h_c A} \quad (8)$$

where h_c is the convective heat transfer coefficient

A is the heat transfer surface area

The heat transfer surface area is the cylindrical face in contact with the fluid

$$A = 2\pi r L \quad (9)$$

where r is the radius of the cylindrical face exposed to heat transfer with the fluid

L is the length of the cylindrical face (i.e. the length of the grid block)

For forced internal convection within pipes, the convective heat transfer coefficient can be expressed in terms of the non-dimensional Nusselt number:

$$h_c = \frac{Nu \cdot k}{D_{\mathrm{h}}} \quad (10)$$

where Nu is the Nusselt number

k is the thermal conductivity of the fluid

D_h is the hydraulic diameter of the pipe

The Nusselt number can be calculated from several published correlations and will generally depend on the flow regime of the fluid within the pipe, the Reynolds number, the Prandtl number, and the Darcy friction factor (depending on the correlation). For brevity, the various Nusselt number correlations are not included here. For the models presented, turbulent pipe flow is handled with the Gnielinksi correlation for Nusselt number.

Substituting the above into Equation (8) gives the final expression for the convective thermal resistance between a fluid and the pipe wall:

$$R_{\text{conv}} = \frac{1}{\pi Nu k L} \quad (11)$$

By substituting in values of k and Nu that correspond to the drill pipe fluid, and annular fluid, the convective thermal resistance on the inside and outside of the drill pipe can be determined.

The conductive resistance through the drill pipe wall can be calculated if the bulk drill pipe thermal conductivity is known:

$$R_{\text{cond}} = \frac{\ln\left(\frac{r_o}{r_i}\right)}{2\pi k_{\text{dp}} L} \quad (12)$$

where r_o is the outer radius of the drill pipe

r_i is the inner radius of the drill pipe

k_{dp} is the bulk thermal conductivity of the drill pipe

The heat transfer rate between the rock and the annular fluid, $\dot{Q}_{\text{rock}}$, is not as trivial to define. As described in Toews et al. (2021) an analytical equation can be derived to estimate the amount of heat transfer from the rock to the wellbore. The equation is analogous to the approach developed by Ramey (Ramey, 1962), and expanded on by Hasan and Kabir (Hasan et al., 1994), for vertical wellbore under the key assumption that the heat transfer can be treated as pseudo-steady state radial heat conduction from the rock into the fluid flowing through the wellbore.

The steady-state radial heat conduction equation is given by:

$$\dot{Q}_{\text{rock}} = \frac{2\pi k_{\text{r}} L (T_{\text{r}} - T_{\text{w}})}{\ln\left(\frac{r_{\text{eff}}}{r_{\text{w}}}\right)} \quad (13)$$

Where k_{r} is the thermal conductivity of the rock formation

T_{r} is the temperature of the undisturbed surrounding rock

T_{w} is the temperature of the wellbore rockface

r_{eff} is the effective thermal radius

r_{w} is the radius of the wellbore/open hole

The steady-state heat conduction is based on an effective thermal radius, r_{eff}, for the rock beyond which the temperature of the rock is unchanged. The effective radius varies with flowing time and is governed by the dimensionless Fourier number, Fo. For this radial conduction problem:

$$\text{Fo} = \frac{\alpha_{\text{r}} t}{r_{\text{eff}}^2} \quad (14)$$

Where α_{r} is the thermal diffusivity of the rock; $\alpha_{\text{r}} = \frac{k_{\text{r}}}{\rho_{\text{r}} C_{p,\text{r}}}$

ρ_{r} is the density of the rock

$C_{p,\text{r}}$ is the specific heat capacity of the rock

The Fourier number is assumed to be constant for this transient heat transfer problem with the prescribed geometry. The constant Fourier number was determined from a least-square regression against an Eavor-internal 3D, numerical, transient radial heat transfer computational fluid dynamics (CFD) model. Equation (14) can be re-arranged in terms of the effective radius, and then substituted into Equation (13):

$$\dot{Q}_{\text{rock}} = \frac{2\pi k_{\text{r}} L(T_{\text{r}} - T_{\text{w}})}{\ln\left(\frac{\sqrt{\frac{\alpha_{\text{r}} t}{\text{Fo}}}}{r_{\text{w}}}\right)} \quad (15)$$

It should be noted that the convective heat transfer coefficient is very high for the fluid in the wellbore compared to the thermal resistance of the rock. Therefore, the temperature of the wellbore rockface, T_{w}, is essentially the same as the bulk fluid temperature, T_{f}, at a given axial location, i.e. $T_{\text{w}} \approx T_{\text{f}}$.

For the drilling problem presented in this paper, the circulation time, t, experienced by the rock will vary with depth – shallower parts of the well will undergo additional circulation time relative to deeper sections of the well. The circulating time can be expressed as a function of measured depth and an average rate-of-penetration (ROP).

$$t = \frac{MD_{\text{well}} - MD_j}{ROP} \quad (16)$$

where MD_{well} is the measured depth to the bottom of the hole

MD_j is the measured depth location of the j^{th} grid block

ROP is the average rate of penetration over the well

In this model, the drilling fluid properties are linear, least-square regressions derived for working fluid properties obtained from NIST Refprop (National Institute of Standards and technology, 2020) as a function of temperature and pressure. When discretizing the model, the axial grid spacing is maintained sufficiently small to ensure that temperature and pressure changes between grid blocks is minimal, maintaining the validity of the assumption of constant thermophysical properties within each grid block. The use of these fluid property regressions makes it straight forward to implement the steady-state model in a spreadsheet program such as Microsoft Excel.

Substituting the fluid property regressions and the annular heat transfer rate (Equation (6)) into the conservation of energy equation for the generic drill pipe grid block (Equation (4)), yields

$$\dot{m}h(T_{\text{dp},j-1}, p_{\text{dp},j-1}) + \frac{T_{\text{dp},j} - T_{\text{ann},}}{R_{\text{ann}}} + \dot{m}g\left(z_j - z_{j-1}\right) = \dot{m}h(T_{\text{dp},j}, p_{\text{dp},j}) \quad (17)$$

Similarly, substituting the fluid property regression, annular heat transfer rate (Equation (6)) and rock heat transfer rate (Equation(15)) into the conservation of energy equation for the generic annulus grid block (Equation (5)) gives

$$\dot{m}h(T_{\text{ann},j+1}, p_{\text{ann},j+1}) + \frac{2\pi k_{\text{r}} L(T_{\text{r},j} - T_{\text{ann},j})}{\ln\left(\frac{\sqrt{\frac{\alpha_{\text{r}} t}{\text{Fo}}}}{r_{\text{w}}}\right)} = \dot{m}h(T_{\text{ann},j}, p_{\text{ann},j}) + \frac{T_{\text{dp},j} - T_{\text{ann},j}}{R_{\text{ann}}} + \dot{m}g\left(z_{j+1} - z_j\right) \quad (18)$$

The fluid property regressions can also be substituted into the simplified conservation of momentum Equations (2), and (3).

After the derivations we are left with four equations for a single *j*-section – two for each grid block – with the majority of the variables dependent on the temperature and pressure from the *j-1* grid blocks (see summary table below). As explained in the next section, the boundary conditions, user defined inputs, and simplifying assumptions allow for the solution of the pressure and temperatures in the drill pipe and annulus.

Table 2: Summary of governing equations for steady-state model

#	Equation	Expression
(2)	Drill pipe conservation of momentum	$p_{\mathrm{dp},j-1} - p_{\mathrm{dp},j} = \left(f_{\mathrm{D}} \cdot L \cdot \frac{\rho_{\mathrm{dp},j-1}}{2} \cdot \frac{{v_{\mathrm{dp},j-1}}^2}{D_{\mathrm{H}}}\right) - \left(\rho_{\mathrm{dp},j-1} \cdot g \cdot \left(z_j - z_{j-1}\right)\right)$
(3)	Annulus conservation of momentum	$p_{\mathrm{ann},j-1} - p_{\mathrm{ann},j} = -\left(f_{\mathrm{D}} \cdot L \cdot \frac{\rho_{\mathrm{ann},j-1}}{2} \cdot \frac{{v_{\mathrm{ann},j-1}}^2}{D_{\mathrm{H}}}\right) - \left(\rho_{\mathrm{ann},j-1} \cdot g \cdot \left(z_j - z_{j-1}\right)\right)$
(17)	Drill pipe conservation of energy	$\dot{m}h(T_{\mathrm{dp},j-1}, p_{\mathrm{dp},j-1}) + \frac{T_{\mathrm{dp},j-1} - T_{\mathrm{ann},j-1}}{R_{\mathrm{ann},j}} + \dot{m}g\left(z_j - z_{j-1}\right) = \dot{m}h(T_{\mathrm{dp},j}, p_{\mathrm{dp},j})$
(18)	Annulus conservation of energy	$\dot{m}h(T_{\mathrm{ann},j}, p_{\mathrm{ann},j}) + \frac{2\pi k_{\mathrm{r}} L(T_{\mathrm{r},j} - T_{\mathrm{ann},j-1})}{\ln\left(\frac{\sqrt{\frac{\alpha_{\mathrm{r}} t}{\mathrm{Fo}}}}{r_{\mathrm{ann}}}\right)} = \dot{m}h(T_{\mathrm{ann},j-1}, p_{\mathrm{ann},j-1}) + \frac{T_{\mathrm{dp},j-1} - T_{\mathrm{ann},j-1}}{R_{\mathrm{ann},j}} + \dot{m}g\left(z_j - z_{j-1}\right)$

2.3 Solution Scheme

When we consider the four equations at each *j*-section, if we assume that the temperature and pressures from the $j-1$ blocks/section are known, then we have a system of 4 equations with four unknowns:

Table 3: Steady-state model system of equations and unknown parameters

Equations	Unknowns
Drill pipe block conservation of momentum	Drill pipe pressure, $p_{\mathrm{dp},j}$
Annulus block conservation of momentum	Annulus pressure, $p_{\mathrm{ann},j}$
Drill pipe block conservation of energy	Drill pipe temperature, $T_{\mathrm{dp},j}$
Annulus block conservation of energy	Annulus temperature, $T_{\mathrm{ann},j}$

The other variables that appear in the four governing equations can be determined from the user defined inputs:

Table 4: Steady-state model known quantities, and parameters

Variable	Source
D_h, hydraulic diameter	• Drill pipe and open-hole/annulus diameters are user specified
f_D, Darcy friction factor	• Can be determined from published correlations which are generally functions of roughness and hydraulic diameters. • Roughness is a user input
v_{dp}, drill pipe fluid velocity v_{ann}, annular fluid velocity	• Calculated from the fluid density (from j-1 block temperature, and pressure), pipe/hole cross-sectional areas, and mass flow rate • Mass flow rate is a user input
z, vertical depth	• The vertical depth of each grid block is a user input (i.e. grid definition)
k_{r}, rock thermal conductivity	• User input
$T_{\mathrm{r},j}$, rock temperature	• The thermal gradient and surface temperature are specified by the user • The vertical depth of each *j*-coordinate can be used to calculate the virgin rock temperature
α_{r}, rock thermal diffusivity	• User defined
t, rock time exposed to flow	• Depends on the ROP and the grid definition – all user inputs
Fo, Fourier number	• Determined from a regression on Eavor-internal CFD simulation results
r_{ann}, radius of the open hole/annulus	• User defined
$R_{\mathrm{ann},j}$, thermal resistance between the annular fluid and drill pipe fluid	• Combination of the convective and conductive resistances • Convective thermal resistances are a function of Nusselt number and fluid thermal conductivity. Nusselt number can be determined from published correlations and using the T/P from the *j-1* blocks. Thermal conductivity of the fluid can be based on T/P from the *j-1* blocks. Convective resistances determined for both drill pipe and annulus blocks • Conductive thermal resistance through the drill pipe wall is user specified. User can specify an average thermal resistance per unit length, or an average thermal conductivity and pipe dimensions

Since the solution of the *j* temperatures and pressures depend on the solution of the *j-1* temperatures and pressures, if we can determine the temperature and pressures at j = 0 (i.e. the boundary conditions for this 1D system), the rest of the system can be solved going from j = 0 (top of the well) to j = n (bottom of the well).

The boundary conditions that are required to solve this system are listed below:

$T_{\mathrm{dp},j=0}$ The inlet temperature to the drill pipe. A constant, user specified value

$p_{\mathrm{dp},j=0}$ The standpipe pressure / injection pressure. Unknown, and a function of the total system pressure drop and the back-pressure

$T_{\mathrm{ann},j=0}$ The return temperature of the drilling fluids. Unknown. Since we have imposed a steady-state assumption on the energy equation, and ignoring the fluid kinetic energy, it follows that the enthalpy of the return fluid is the sum of the enthalpy of the inlet fluid and the total specific heat transfer from the rock to the wellbore system (i.e. $\frac{\dot{Q}_{\mathrm{rock}}}{\dot{m}}$). The temperature of the return fluid can be back-calculated from the enthalpy regression, and $p_{\mathrm{ann},j=0}$ (which is known/user inputted).

$p_{\mathrm{ann},j=0}$ Back/return pressure (MPD if applicable). A constant, user specified value

Two of the four boundary conditions are not known prior to solving the system. To solve the system, an iterative "guess-and-check" solution method is employed. The steps in the iterative solver are summarized in the numbered list below:

1. Start with guesses for the two unknown boundary conditions ($p_{\mathrm{dp},j=0}$, $T_{\mathrm{ann},j=0}$)
2. Starting at j = 1 (first/top grid block),
    - Solve the pressures in the drill pipe and annulus from the two conservation of momentum equations

- Solve the fluid temperatures in the drill pipe and annulus from the two conservation of energy equations (it should be noted that the quadratic formula is required to calculate the fluid temperature from the enthalpy regressions)

Take the T/P solutions and use them in the solution of the next j-section. Repeat for all grid blocks / j-sections going to the bottom of the well

3. Once the system has been solved, calculate the actual values for two boundary conditions that were originally guessed. Determine the error between the guess values and the calculated values.
4. Using a root-finding or optimization algorithm (such as Newton's method) iteratively update the guess for the boundary conditions based on the most recent iteration's error.
5. Iterate until the error is within some user specified tolerance, or a maximum number of iterations has been reached.

The discretized steady state model has been implemented in Microsoft Excel, and the iterative solution routine is written in VBA using a modified Newton's method. On average, the model only takes a few seconds to converge on the correct answer.

2.4 Model Case Study Results & Validation

The discretized steady state model is a quick and flexible way of modelling the drill pipe and annular circulating fluid temperatures. The discretized nature of the model allows for complex well trajectory, rock temperature profiles, and drill pipe designs to be modelled and their impacts on circulating temperatures/pressures evaluated.

The results presented in this section serve two purposes: (1) illustrate the typical results of the steady state model, and (2) summarize the impacts of a thermally resistive drill pipe (a.k.a. IDP, insulated drill pipe) on circulating temperatures.

The table below summarizes the model inputs for two hypothetical drilling cases.

Table 5: Steady-state model case descriptions

Model Input	Units	Case 1: Carbon Steel (CS) String	Case 2: Hypothetical IDP String
Fluid Properties			
Inlet Temperature (Constant tank temperature assumed)	°C	30	30
Annulus back pressure	kPag	0	0
Pump rate	m3/min	2.50	2.50
Well Trajectory & Grid Definition			
Well depth	m	5,000	5,000
Deviation (from vertical)	°	0	0
# of grid blocks (j-dir)	#	500	500
Grid block size	m	10	10
Geology			
Surface Temperature	°C	10	10
Geothermal Gradient	°C/km	50	50
Rock conductivity	W/mK	2.5	2.5
Rock density	kg/m3	2,700	2,700
Rock specific heat capacity	J/kgK	790	790
Well Design / Size			
Drill pipe ID	mm	121.4	121.4
Drill pipe OD	mm	139.7	139.7
Open hole diameter	mm	215.9	215.9
Drill pipe roughness	mm	0.05	0.05
Open hole roughness	mm	0.05	0.05
Drill pipe conductive resistance	mK/W	5.08×10^{-4}	**1.0×10^{-2}**
Drilling Rig			
Rate-of-penetration (ROP)	m/hr	12.0	12.0

- *In this example, no casing strings and cement are modelled (however, the model can accommodate thermal impacts of casing and cement via thermal resistance inputs for each well segment)*
- *In case 2, the bottom 100m of the drill string (10 blocks) is modelled with full carbon steel drill pipe to emulate the BHA which has very little thermal resistance*
- *Pressure drop across the BHA components not explicitly modelled*

Figure 4 below shows the main outputs of the steady state model – the pressure and temperatures in the drill string and annulus along the entire well path – for case 1.

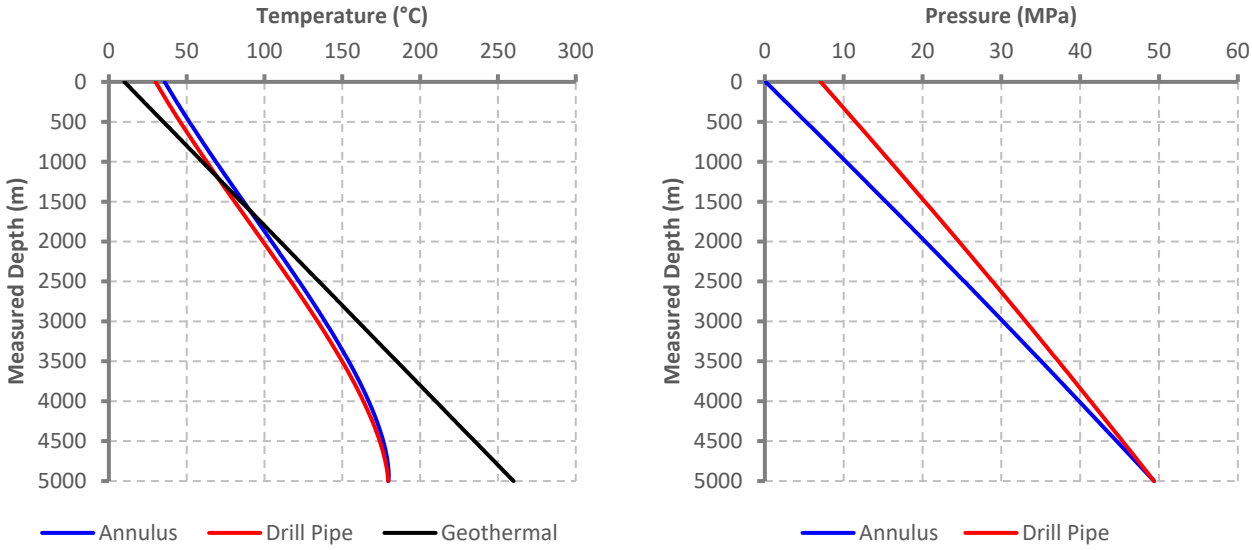

Figure 4: Steady-state model results for case 1

Although the primary outputs of the model are the circulation temperature and pressure, since the model has been discretized and implemented in a spreadsheet model, it is possible to interrogate the variation in intermediate parameters and calculated quantities such as the heat transfer between the annulus and drill pipe along the drill string.

These model results can give the user an idea of the feasibility of drilling various HPHT wells. The maximum downhole circulating temperatures, and estimated standpipe pressures may be used to refine the design of HPHT wells based on known thermal limitations of the BHA components, and/or rig pump capacities.

For example, the model can be used to evaluate the impacts on drilling with a drill string that has a significantly higher thermal resistance relative to standard drill pipe. It is recognized by the authors that the drill pipe thermal resistance included in case 1 does not account for the various coatings typically found on a standard joint of drill pipe. The figure below illustrates the impact on circulating temperatures when changing the drill string design.

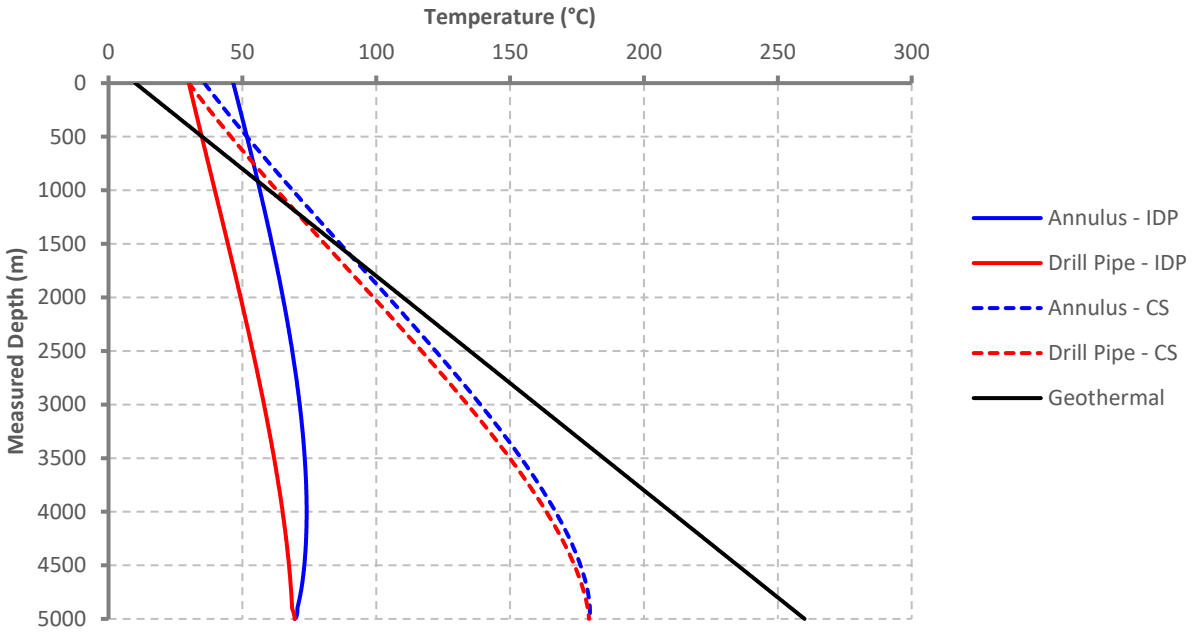

Figure 5: Steady-state model results comparison for carbon steel (CS) drill pipe and a hypothetical insulated drill pipe (IDP)

In this theoretical comparison, the maximum downhole circulating temperature for case 1 and 2 are, 178.7 °C and 73.6 °C, respectively. Typical temperature-sensitive components have limits of ~150 °C. The carbon steel drill pipe would not enable the successful drill and completion of this 5 km HPHT well. However, with an IDP drill string, the model suggests a successful well – keeping the circulating temperatures much below the threshold of common temperature critical components.

To validate the steady-state model, it was compared against Hasan and Kabir's (1996) analytical model for forward circulation (flow down the drill pipe). Since the analytical model assumes that the time exposed to flow does not vary with depth, and constant fluid properties, the steady-state model was adapted to closely replicate the assumptions in the analytical model.

Other than the adaptations to the steady-state model, the results shown in Figure 6 and Figure 7 below use the same inputs as case 1 from Table 5. The figures compare the steady-state model against the analytical solutions for flowing times of 24 hours, and 7 days (168 hours).

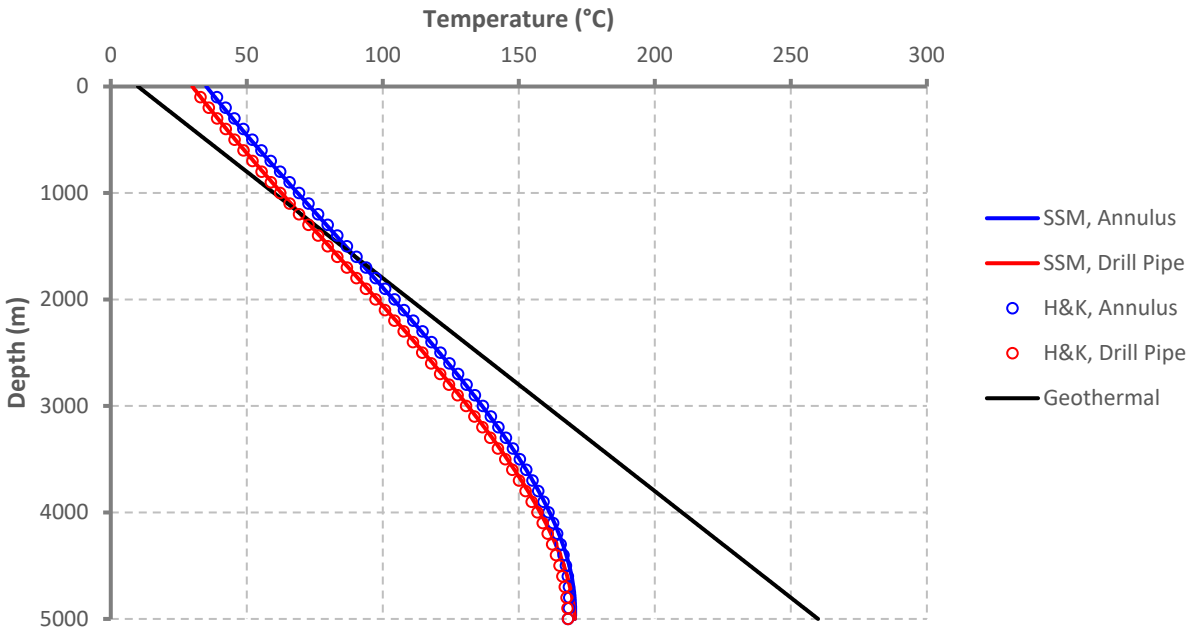

Figure 6: Steady-state model validation with Hasan & Kabir forward circulation analytical mode (case1, flowing time of 24 hours).

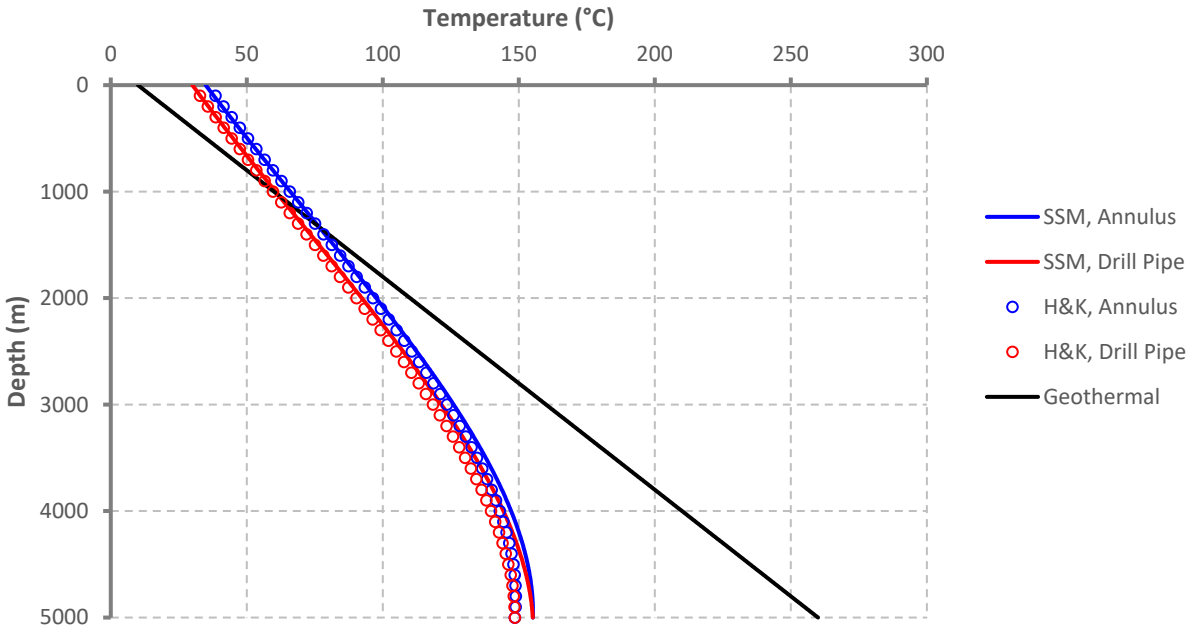

Figure 7: Steady-state model validation with Hasan & Kabir forward circulation analytical model (case 1, flowing time of 168 hours).

The steady-state model slightly overpredicts the fluid temperatures. The error generally gets larger as the flowing time increases. The average different between the steady-state model and the analytical model is 0.6%, 2.1% in Figure 6, and Figure 7, respectively. In general, there is good agreement between the steady-state and analytical models.

2.5 Parameter Sensitivities

Because the steady state model is quick to converge to a solution, it can be used to rapidly run a variety of sensitivities to understand the impact of various parameters on the outputs of the model. Presented below is a simple tornado plot summarizing the impact of the variance in key model inputs. Each bar in the tornado plot represents the change in the maximum circulating temperature in the wellbore with a +/- 10% change in the respective model input. It should be noted that the likelihood of a +/- 10% change in each model input is not conveyed with a tornado chart as simple as the one shown in Figure 8.

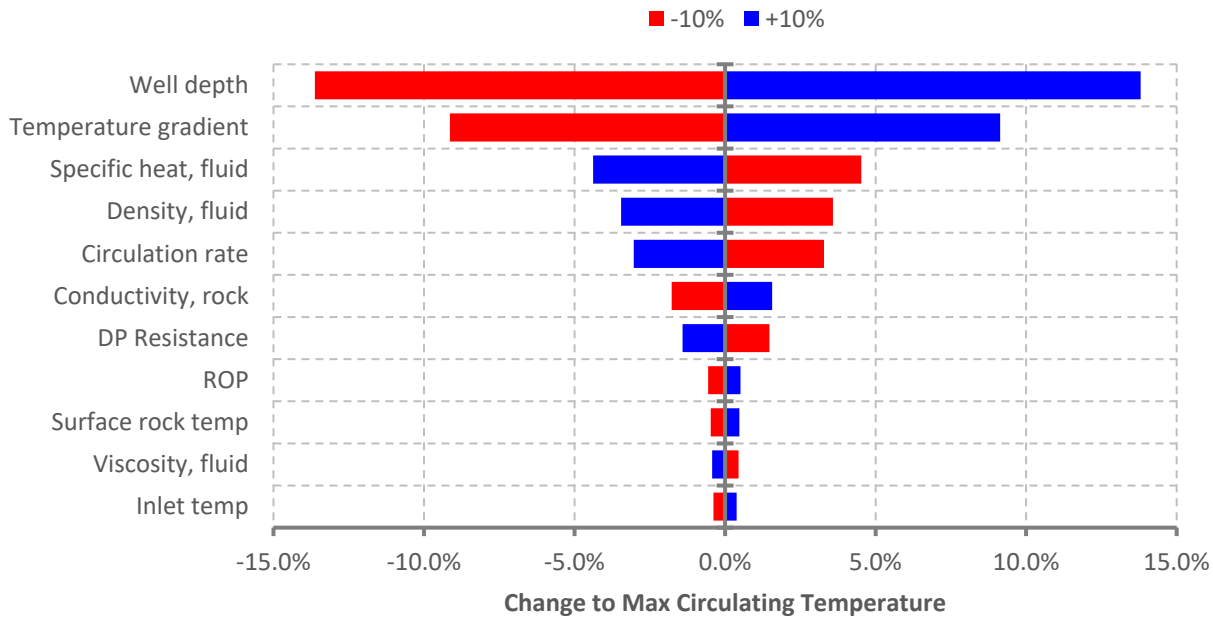

Figure 8: Sensitivity of maximum downhole circulation temperature with model inputs (case 1)

In order of most impactful to least impactful model inputs:

1. Well design inputs
    i. Well depth (i.e. TD)
2. Geological inputs
    i. Geothermal (temperature) gradient
    ii. Rock conductivity
3. Drilling mud/fluid inputs
    i. Specific heat
    ii. Density
    iii. Viscosity (to a lesser extent)
4. Drilling Rig inputs
    i. Circulation Rate
5. Drill string inputs
    i. Drill pipe thermal resistance

Although modifying the mud design could improve wellbore cooling during circulation, factors other than circulating temperature are typically prioritized when designing a mud blend. Higher circulation rates can reduce circulating temperatures; however, rates are limited by the maximum flow rates through the BHA, as well as pressure and rate limitations of surface equipment. That leaves the drill pipe resistance as being one of the few levers available to the well design team to influence the circulating temperatures.

Relative to the impact of well depth and geothermal gradient, the circulating fluid temperature is less sensitive to the thermal resistance of the drill pipe. In order to accommodate a deeper well, or a higher geothermal gradient, the drill pipe thermal resistance needs to increase at least an order of magnitude more than the change in depth or gradient.

2.6 Drill Pipe Technology Limits

Assuming that the drill pipe can be engineered to achieve a range of thermal resistances, the steady-state model can be used to determine the maximum drillable depths for a given geothermal gradient for a fixed maximum circulating temperature (i.e. the temperature limitations of the BHA components).

For illustrative purposes, the same 5-1/2” drill pipe designs in cases 1 and 2 above are considered:

Table 6: Drill pipe designs

Description	Base Pipe (ID x OD)	Thermal Resistance (mK/W)
Bare Carbon Steel	121.4 x 139.7	5.08×10^{-4}
Hypothetical IDP	121.4 x 139.7	1.00×10^{-2}

IDP constructions with varying insulative layers was explored by Finger et al. (2000).

When coupled with the steady-state model, the maximum drillable depths for each of the drill string designs can be determined (temperature considerations only). Other model inputs are consistent with those in Table 5, and the maximum allowable bottomhole circulating temperature of 150 °C is assumed.

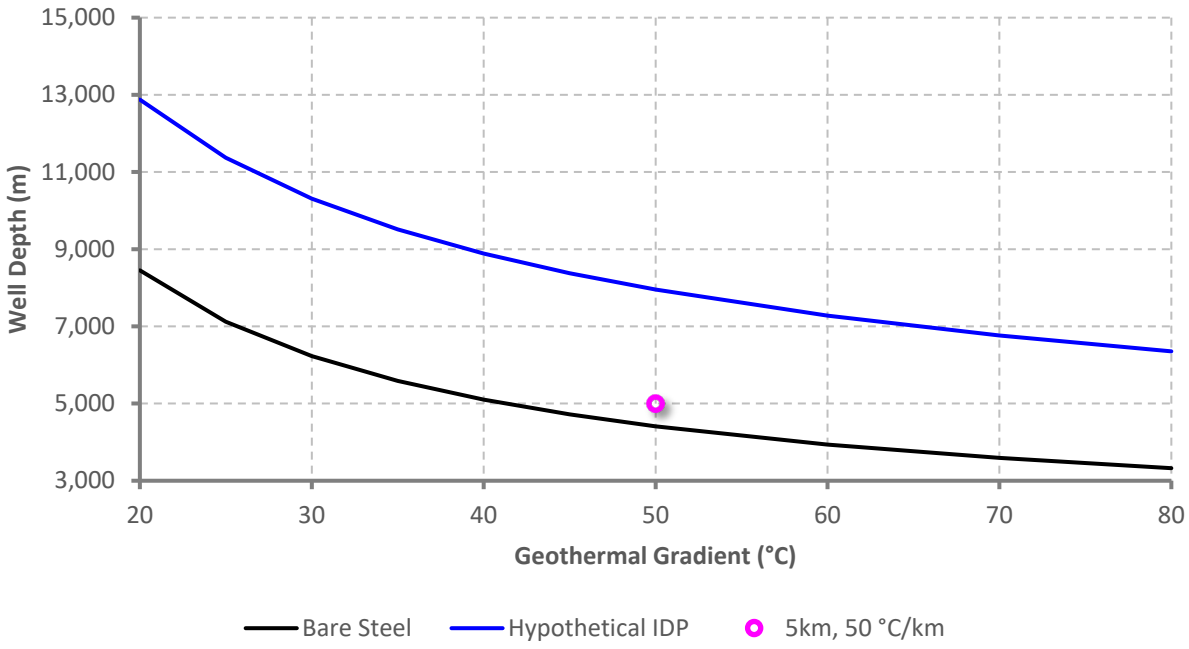

Figure 9: Max drillable well depths for the illustrative drill pipe designs

The regions under each of the lines represent the gradient-depth combinations that can be feasibly drilled with a given drill pipe design.

Visualized in another way, the corresponding drillable bottom-hole rock temperatures (BHRT) for each string design can be plotted.

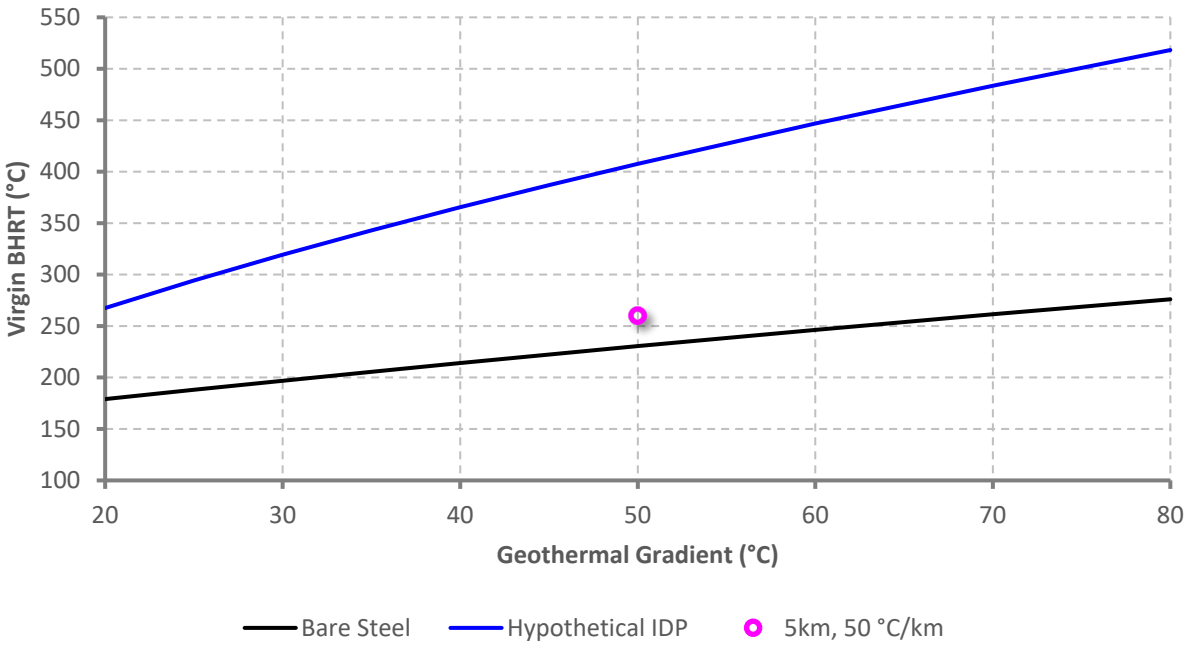

Figure 10: Max drillable bottom-hole rock temperatures for the illustrative drill pipe designs

As mentioned above, the economics of a MCLGS improves with increasing BHRT. By incorporating an insulated drill pipe into a drilling program, higher rock temperatures can be drilled and exploited, improving the overall project economics and prospective investor returns. The figures above also confirms that drill pipe resistances need to change by orders of magnitude in order to materially influence bottom-hole circulating temperatures.

3. TRANSIENT MODEL

The steady-state model provides a wellbore temperature and pressure solution that only represents a "snapshot" in time. However, during the normal drilling of a geothermal well, there are transient operations that cannot be properly modelled by a pseudo steady state model. For example, some transient events that should be modelled to understand their impacts on wellbore temperatures are:

- Connections,
- Formation kicks,
- Loss of circulation,
- Running/tripping in hole,
- Pulling/tripping out of hole,
- Changes in circulation rate with time, and
- Changes in inlet temperature with time

The transient model presented in this section takes a comparatively more rigorous approach to modelling. The transient model employs a numerical solution of the transient 2-D heat conduction in the rock surrounding the wellbore coupled with a numerical solution of the transient energy equation for the fluid flow inside the wellbore (drill pipe and annulus).

3.1 Model Formulation

The transient model is a 2-D, discretized rock and wellbore drilling model. A schematic of the transient model is shown in Figure 9.

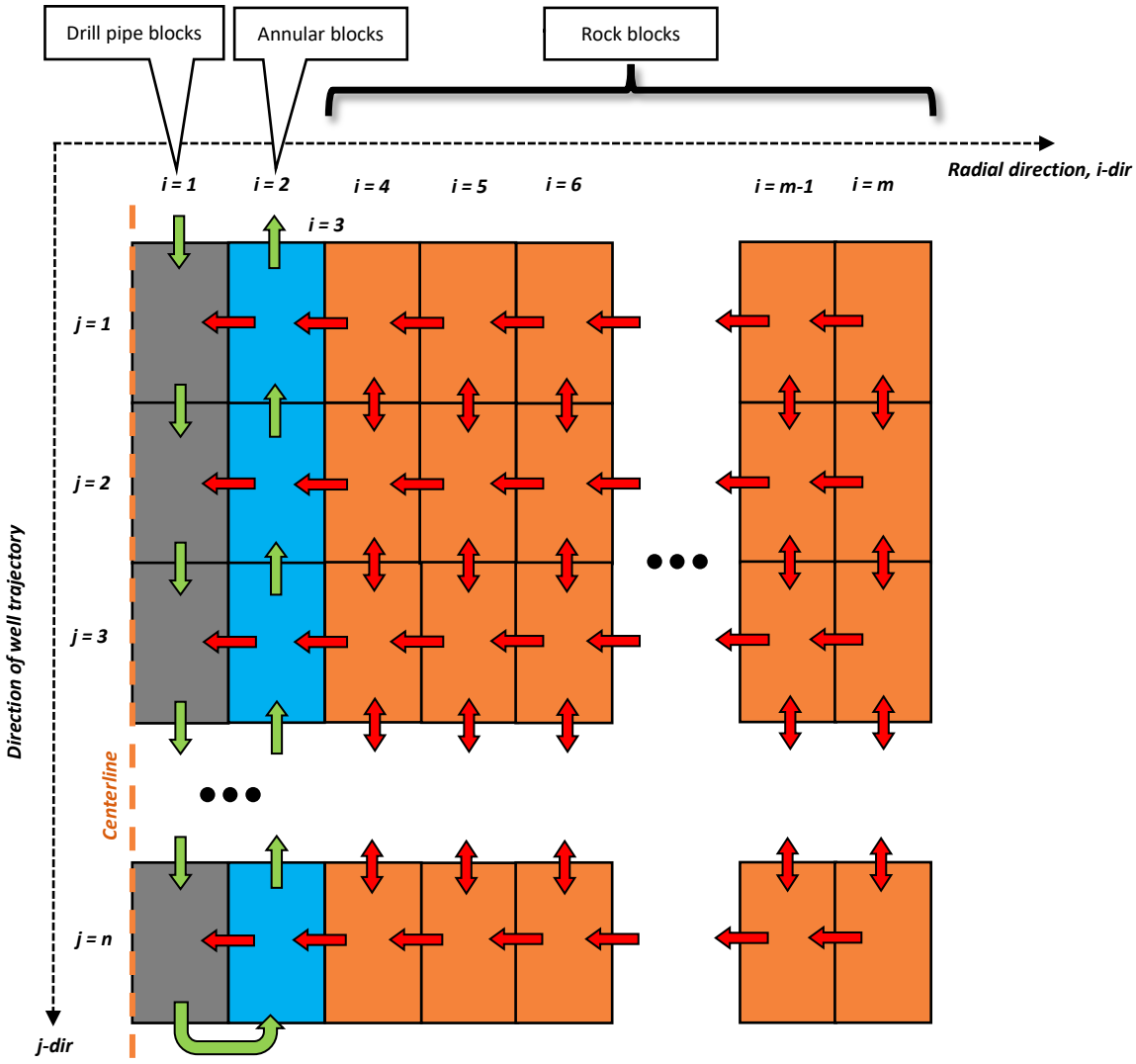

Figure 11: Transient model schematic

Similar to Figure 2 for the steady-state model, the green and red arrows in Figure 9 represent the mass and energy flows within the coupled rock-wellbore system, respectively.

3.2 Governing Equations and Assumptions

3.2.1 Rock Equations

Fourier's Law of Heat conduction and the conservation of energy equation can be combined to derive the partial differential equation (PDE) that governs the transient conduction of thermal energy in rock with a constant thermal conductivity:

$$\rho_{\mathrm{r}} C_{p,\mathrm{r}} \left(\frac{\partial T}{\partial t} + v_r \frac{\partial T}{\partial r} + \frac{v_\theta}{r} \frac{\partial T}{\partial \theta} + v_z \frac{\partial T}{\partial z} \right) = k_r \left(\frac{1}{r} \frac{\partial}{\partial r} \left(r \frac{\partial T}{\partial r} \right) + \frac{1}{r^2} \frac{\partial^2 T}{\partial \theta^2} + \frac{\partial^2 T}{\partial z^2} \right) + \dot{g} \qquad (19)$$

where ρ_{r} is the rock density

$C_{p,\mathrm{r}}$ is the rock specific heat capacity

T is the rock temperature

t is time

v is velocity

r is the radial direction

θ is the angular direction

z is the axial direction

k_{r} is the rock thermal conductivity

$\dot{g}$ is the rate of heat generation

Assuming transient heat transfer by conduction only, and no angular variation in temperature yields:

$$v_r = v_\theta = v_z = 0$$

$$\frac{\partial T}{\partial \theta} = 0$$

$$\dot{g} = 0$$

Equation (19) reduces to:

$$\frac{1}{\alpha_{\mathrm{r}}}\frac{\partial T}{\partial t} = \frac{1}{r}\frac{\partial}{\partial r}\left(r\frac{\partial T}{\partial r}\right) + \frac{\partial^2 T}{\partial z^2} \quad (20)$$

where α_{r} is the thermal diffusivity of the rock: $\alpha_{\mathrm{r}} = \frac{k_{\mathrm{r}}}{\rho_{\mathrm{r}} C_{p,\mathrm{r}}}$

3.2.2 Wellbore Equations

The transient energy equation for the 1D fluid flow in the wellbore along the axial coordinate system can be expressed for both the fluid in the drill pipe, and the annular space:

Annular fluid: $$\frac{\partial \rho_{\mathrm{f,ann}} e_{\mathrm{ann}}}{\partial t} + \frac{\partial G(h_{\mathrm{ann}} + gy)}{\partial z} = U_{\mathrm{rockface}}\left(T_{\mathrm{wr}} - T_{\mathrm{f,ann}}\right) + U_{\mathrm{dp}}\left(T_{\mathrm{f,dp}} - T_{\mathrm{f,ann}}\right) \quad (21)$$

Drill pipe fluid: $$\frac{\partial \rho_{\mathrm{f,dp}} e_{\mathrm{dp}}}{\partial t} + \frac{\partial G(h_{\mathrm{dp}} + gy)}{\partial z} = U_{\mathrm{dp}}\left(T_{\mathrm{f,ann}} - T_{\mathrm{f,dp}}\right) \quad (22)$$

where $\rho_{\mathrm{f,ann}}$ is the fluid density in the annulus

$\rho_{\mathrm{f,dp}}$ is the fluid density in the drill pipe

e_{ann} is the internal energy of the fluid in the annulus

e_{dp} is the internal energy of the fluid in the drill pipe

G is the mass flux of the fluid flowing through the wellbore

h_{ann} is the enthalpy of the fluid in the annulus

h_{dp} is the enthalpy of the fluid in the drill pipe

g is the constant due to the acceleration due to gravity

y is the position in the vertical direction (parallel to gravity)

z is the axial direction

U_{rockface} is the heat transfer coefficient from the rock/wellbore boundary to the fluid

U_{dp} is the heat transfer coefficient between the annular fluid and the drill pipe fluid

T_{wr} is the temperature of the rock at the rock/wellbore boundary

$T_{\mathrm{f,ann}}$ is the temperature of the bulk fluid in the annulus

$T_{\mathrm{f,dp}}$ is the temperature of the bulk fluid in the drill pipe

The change in kinetic energy has been neglected in Equations (21) and (22) as this contribution is negligible compared to the internal energy and enthalpy change of the fluid. In addition, the conservation of mass has been invoked for an incompressible fluid so the mass flux, G, is constant in the drill pipe and annulus (although in different directions).

The heat transfer coefficients, U_{rockface} and U_{dp}, are comprised of any conductive resistance between the rock and the wellbore (e.g. casing and cement, and/or drill pipe wall) and convective resistances of the flowing fluids. Similar to the governing equation derivations for the steady-state model, the heat transfer coefficients can be expressed using resistance theory and the standard thermal resistance equations for cylindrical conductive heat transfer, and cylindrical convective heat transfer of a fluid. These equations and their combination to create the total heat transfer coefficients will not be repeated here.

A pseudo-steady state version of the momentum equation is employed whereby the pressure drop of the fluid is calculated using the Colebrook White type correlation. Because of its similarity to the equations detailed for the steady-state model, the simplified conservation of momentum equations are not repeated here.

Ultimately, the following assumptions and simplifications are made to derive the fluid equations above:

1. The change in kinetic energy is neglected
2. A simplified, pseudo-steady version of the momentum equation is employed
3. No impact of the rock cuttings on the fluid properties (e.g. specific heat, density, viscosity)

3.2.3 Initial and Boundary Conditions

The temperature field of the rock at time t = 0 must be specified along with boundary conditions for the temperature, pressure, and flow rate of the fluid at the inlet of the drill pipe. The rock boundary temperature and radius must also be specified. For all simulations, the boundary rock radius is set large enough such that it has not been impacted by the thermal front and the boundary temperature remains at virgin rock temperature.

To couple the sets of wellbore equations and rock equations, the heat flow at the rock-wellbore interface must be continuous such that the Fourier law of heat conduction in the rock at the boundary equals the transfer to the fluid in the annulus.

$$k_{\text{r}} \frac{\partial T}{\partial r} = U_{\text{rockface}}\left(T_{\text{wr}} - T_{\text{f,ann}}\right) \tag{23}$$

3.2.4 Discretization and Numerical Solution

The PDE describing the transient 2-D conduction in the rock can be solved numerically by integrating Equation (20) over a discrete finite control volume, $dV = 2\pi r\, dr\, dz$ and specified time step, Δt:

$$\frac{1}{\alpha_{\text{r}}}\pi\left(r_{i+1}^2 - r_i^2\right)\left(z_{j+1} - z_j\right)\frac{T_{i,j}^{n+1} - T_{i,j}^{n}}{\Delta t} = 4\pi\left(z_{j+1} - z_j\right)\left(r_{i+1}\frac{T_{i+1,j}^{n+1} - T_{i,j}^{n+1}}{r_{i+2} - r_i} - r_i\frac{T_{i,j}^{n+1} - T_{i-1,j}^{n+1}}{r_{i+1} - r_{i-1}}\right) + 2\pi\left(r_{i+1}^2 - r_i^2\right)\left(\frac{T_{i,j+1}^{n} - T_{i,j}^{n}}{z_{j+2} - z_j} - \frac{T_{i,j}^{n} - T_{i,j-1}^{n}}{z_{j+1} - z_{j-1}}\right) \tag{24}$$

Where i indexes the radial direction, j indexes the axial direction (along the wellbore), and n indexes time.

Note that the radial derivatives on the right-hand side of Equation (24) are implicitly calculated at the new time step (n+1) whereas the axial derivatives are explicitly calculated at the previous time step (n). This is acceptable as the typical grid spacing in the axial direction is much larger than the radial direction. Consequently, the stability criterion in the explicit numerical treatment in the axial direction is not violated.

The transient 1D energy equation for the annulus and drill pipe are discretized in the following manner. For the drill pipe:

$$\rho_{\text{f,ann}}\pi\left(r_{\text{ann}}^2 - r_{\text{dp,o}}^2\right)\Delta z\frac{\left(h_{2,j}^{n+1} - h_{2,j}^{n}\right)}{\Delta t} + G\pi\left(r_{\text{ann}}^2 - r_{\text{dp,o}}^2\right)\left(\left(h_{2,j}^{n+1} - h_{2,j+1}^{n+1}\right) + gy\right) = U_{\text{rockface},j}\Delta z\left(T_{3,j}^{n+1} - T_{2,j}^{n+1}\right) + U_{\text{dp},j}\Delta z\left(T_{1,j}^{n+1} - T_{2,j}^{n+1}\right) \tag{25}$$

where the term $U_{\text{rockface},j}\Delta z\left(T_{3,j}^{n+1} - T_{2,j}^{n+1}\right)$ is the heat transfer from the rock to the wellbore. For the annulus:

$$\rho_{\text{f,dp}}\pi r_{\text{dp,i}}^2\Delta z\frac{\left(h_{1,j}^{n+1} - h_{1,j}^{n}\right)}{\Delta t} + G\pi r_{\text{dp,i}}^2\left(\left(h_{1,j}^{n+1} - h_{1,j-1}^{n+1}\right) + gy\right) = U_{\text{dp},j}\Delta z\left(T_{2,j}^{n+1} - T_{1,j}^{n+1}\right) \tag{26}$$

where the term $U_{\text{dp},j}\Delta z\left(T_{2,j}^{n+1} - T_{1,j}^{n+1}\right)$ is the heat transfer from the annulus to the drill pipe fluid.

The discretized wellbore equations above make use of specific enthalpy, h, instead of specific heat capacity and temperature to properly model the Joule-Thomson effect, which has a large impact on temperature change due to pressure drops experienced through the drill bit and the other BHA components.

Thermophysical properties are calculated using NIST Refprop, or the open-source CoolProp library (Bell et al. 2014) (usage will depend on what libraries are installed on the user's local machine).

The governing equations and their discretization are similar to those described by Holmes et al. (2021) for Eavor's transient MCLGS model and have been proven to match field operating data at the Eavor-Lite™ demonstration project. However, unlike the MCLGS model, the system of algebraic equations describing the drill-pipe-annulus-rock system cannot be directly solved using the Tri-Diagonal Matrix

Algorithm (TDMA). Instead, the system of linear equations are divided into three discrete solution routines/steps and iteratively solved until convergence to a user-specified tolerance is met. The three solution routines are described in the section below.

3.3 Solution Scheme

The solution of the large sparse matrix to compute the entire temperature field at the new time-step, $T_{i,j}^{n+1}$, is achieved through iteration to reach convergence.

3.4 Handling Transient Operations

Throughout any major drilling program, many parameters are constantly changing. While drilling, circulation rates are varied, inlet mud temperatures can change due to ambient and return temperatures, and the depth of the drill pipe changes as the well is drilled deeper, and while tripping. The changes in these parameters with time cannot be explicitly handled by the steady-state model. The transient model, however, allows for the manipulation of these key variables with time.

3.4.1 Drilling

During drilling, the following model inputs can be varied with time to account for the changing operations over the life of a program:

- Drill pipe depth (e.g. to model drilling, and tripping in and out of the hole)
- Hole depth
- Inlet mud temperatures (e.g. to model mud cooling, or the change with ambient temperatures throughout the day)
- Mud rheology (e.g. to model changes in mud design over a program)

Additionally, the properties of the full length drill string are defined as a function of measured depth at the start of the simulation. During the simulation, as the drill pipe is moved up and down in the hole, the transient model will account for the change in drill pipe position in the hole following a last-in-first-out methodology. If the thermophysical properties of the drill string vary along its length, the physical implications of their relative location in the well will be explicitly accounted for throughout the duration of the simulation.

3.4.2 Kicks & Lost Circulation

The addition/removal of drilling fluids into/out of the wellbore can also be changed with time to model kicks and periods of lost circulation (LOC). More specifically, the size and rate of a kick, or LOC event can be varied to allow the user to sensitize on the impacts to wellbore temperatures.

3.5 Model Case Study Results and Comparison

The model case study presented below follow the same inputs as described in the steady-state section (for cases 1 and 2), with the following additional transient model related inputs:

Table 7: Additional transient model inputs

Model Input	Units	Value
# of axial grid blocks (j-dir)	#	500
Axial grid block size	m	10
Grid outer radius	m	15
# of radial grid blocks (i-dir)	#	40
Radial grid block size	m	*varies*

Note: the radial direction is discretized such that the radial blocks are growing exponentially away from the well

The run starts with the model drilling at a constant ROP of 12 m/hr, and then once it hits TD at 5,000 m circulates on bottom for the remainder of the simulated time. The tripping of the drill pipe in and out of the hole has been excluded from this simulation intentionally. The steady-state model cannot account for tripping, so to make a direct comparison between the two models, it has been neglected from this transient model run.

Unlike the steady-state model, the transient model is capable of modelling changes in stand-pipe pressure (inlet pressure), inlet temperature, tubing depth and open hole depth with time. This allows for the estimation of temperature and pressure effects due to the normal transience encountered when drilling HPHT geothermal wells.

The figure below shows the time-series input data for the run:

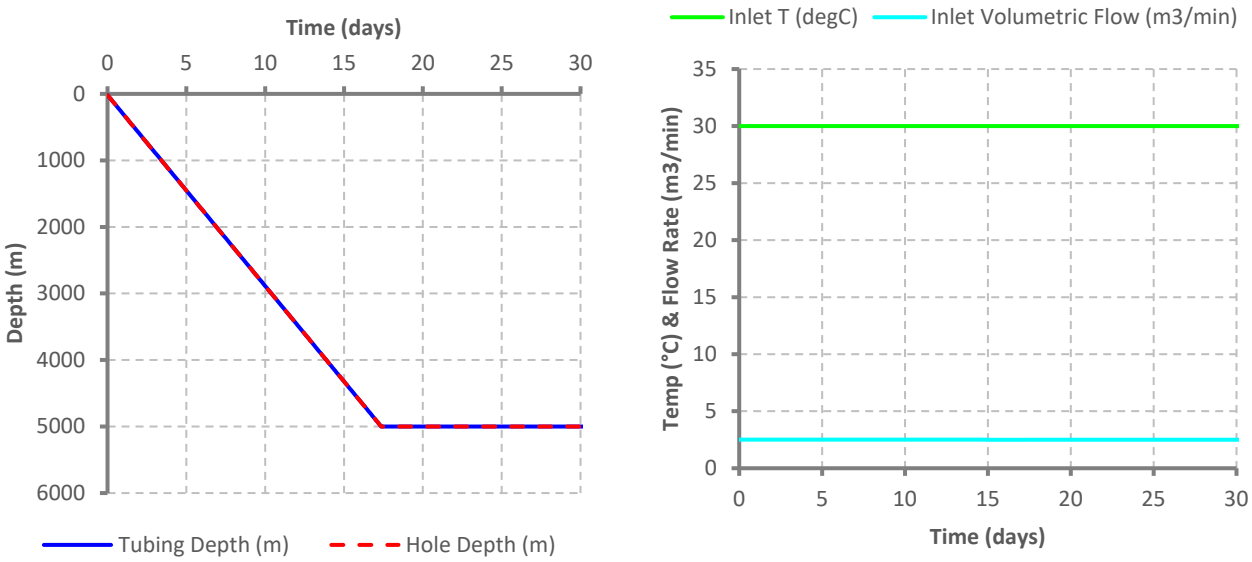

Figure 12: Transient model time-series inputs

The transient drilling model (TDM) reports the pressure and temperature results for each time step. The results can be plotted to show the change in temperature and pressure at specific points in the well (e.g. at temperature-critical component locations) throughout the simulated time, or snapshots of the entire wellbore temperature/pressure profiles at specific points in time.

The figure below shows the variation in temperature and standpipe pressure (SPP) with time, as well as the steady-state model (SSM) solutions for case 1:

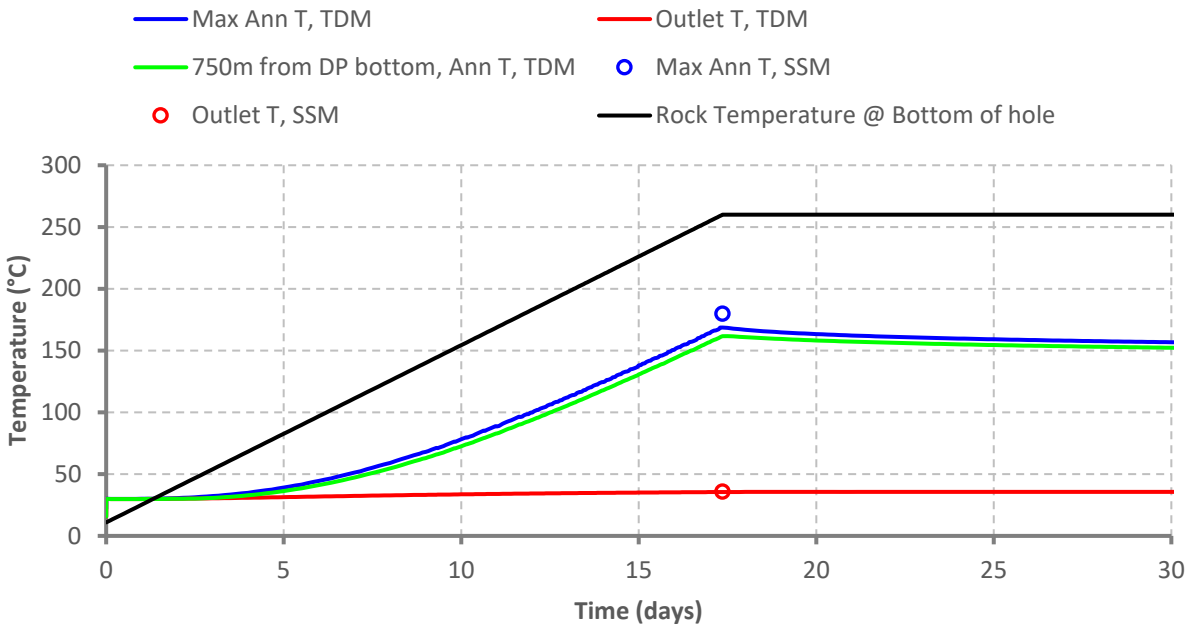

Figure 13: Temperature outputs from transient model (case 1)

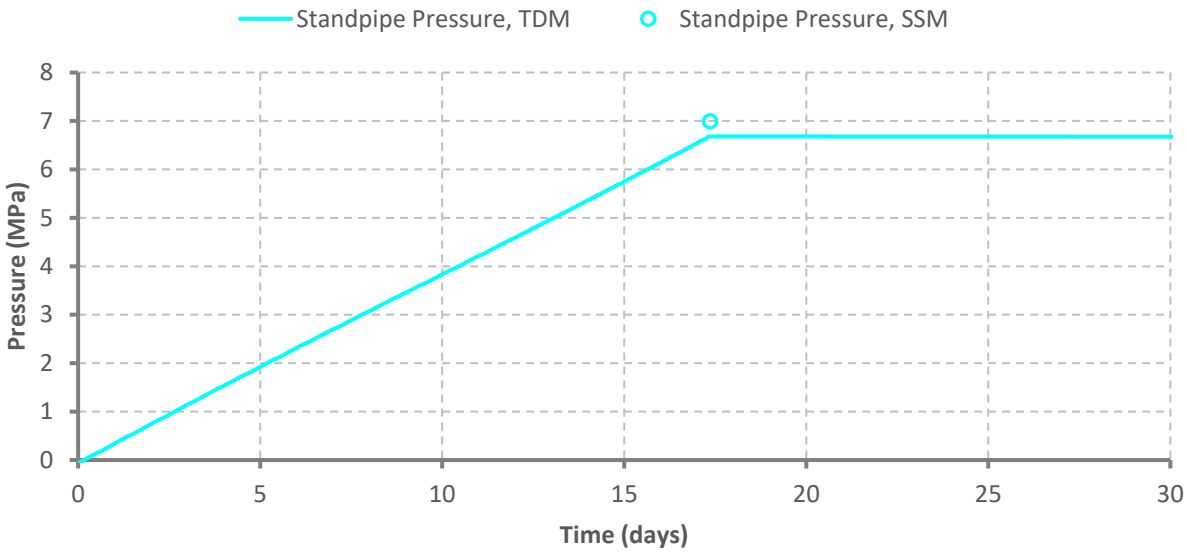

Figure 14: Standpipe pressure output from transient model (case 1)

A comparison of the wellbore temperature and pressure profiles between the two models is shown in the figures below.

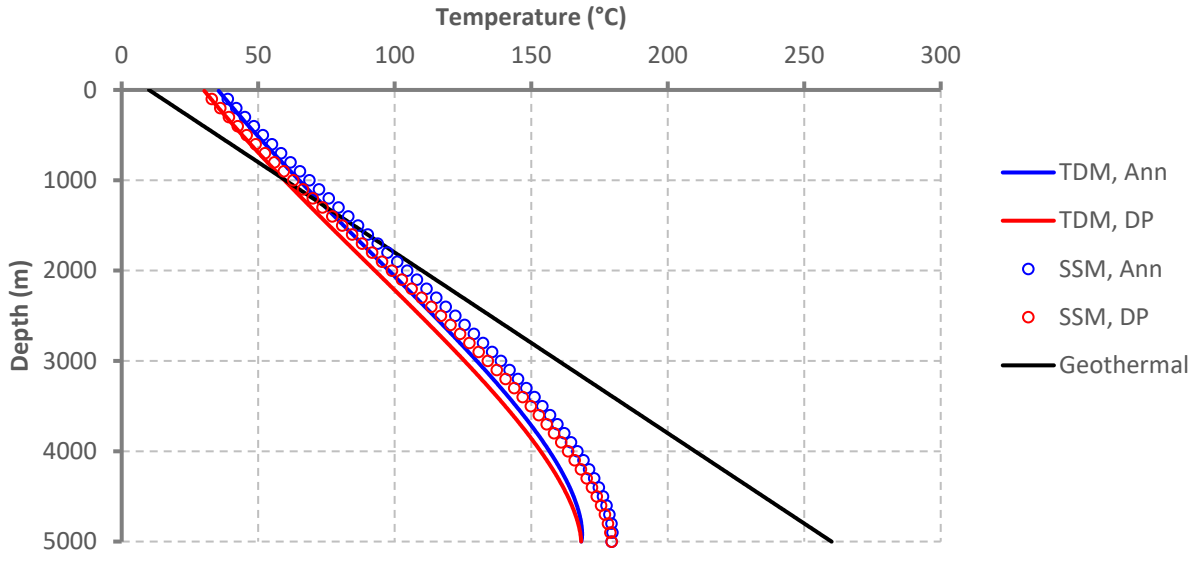

Figure 15: Wellbore temperature solution comparison between transient and steady-state models (case 1)

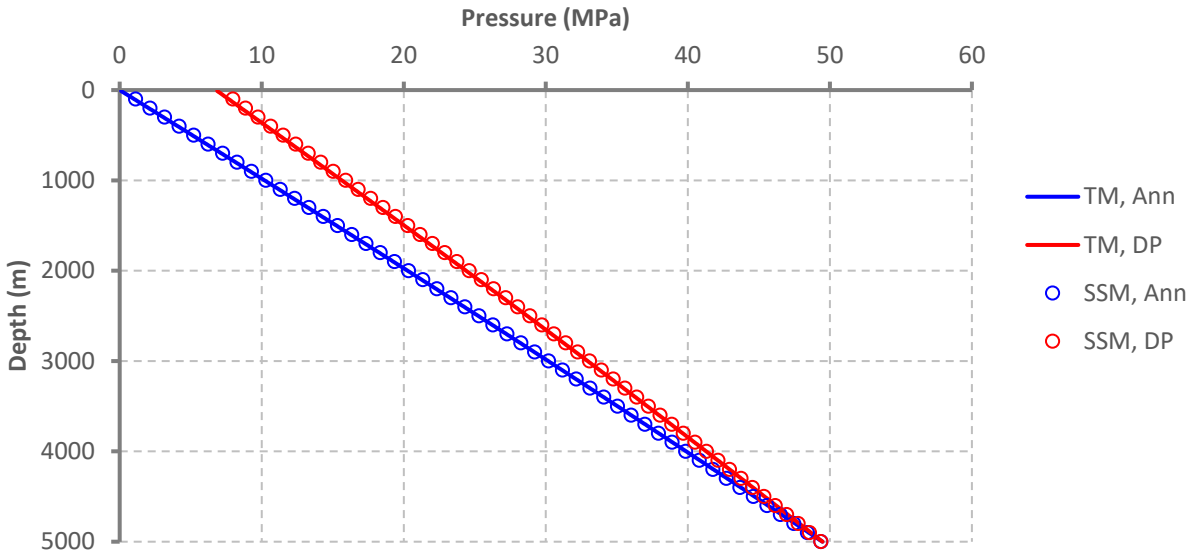

Figure 16: Wellbore pressure solution comparison between transient and steady-state models (case 1)

Case 2 (hypothetical IDP) model results are below:

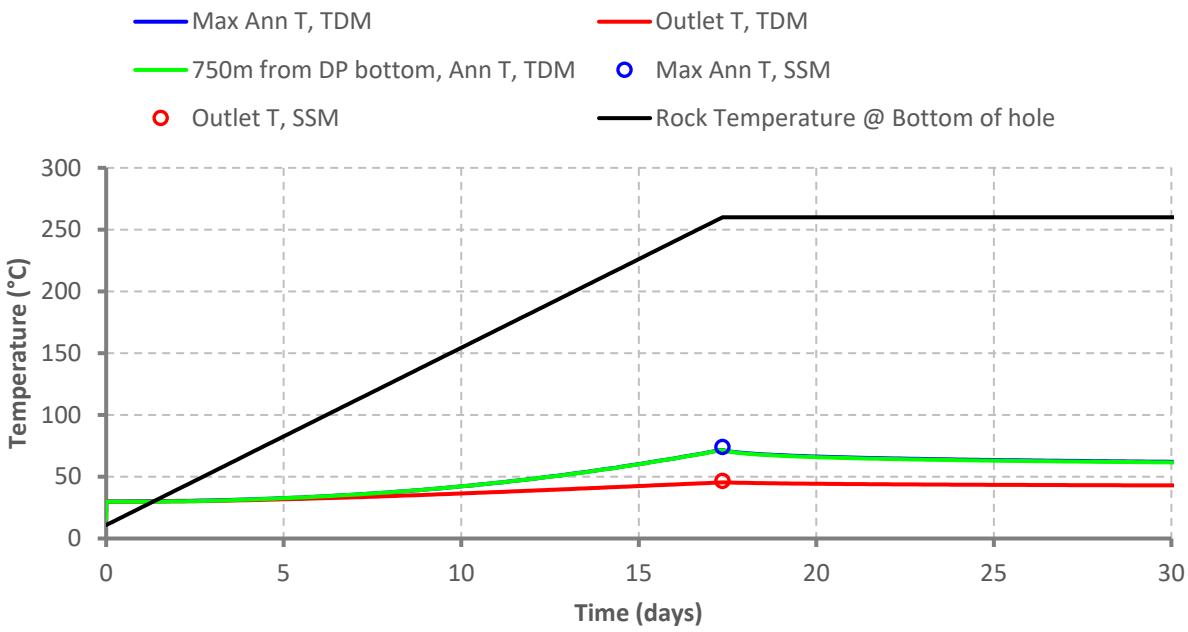

Figure 17: Temperature outputs from transient model (case 2)

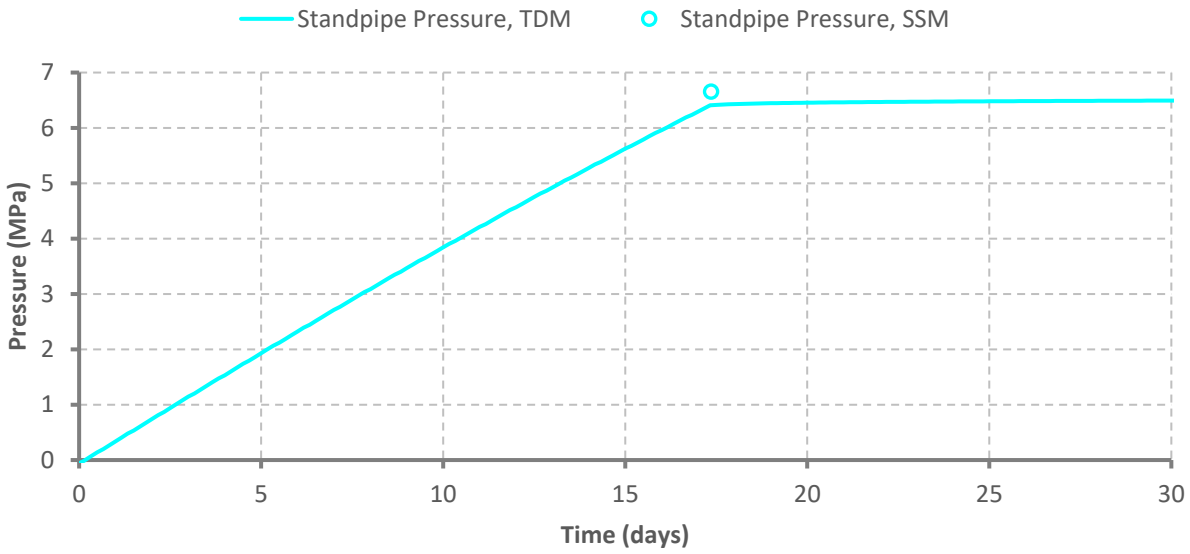

Figure 18: Standpipe pressure output from transient model (case 2)

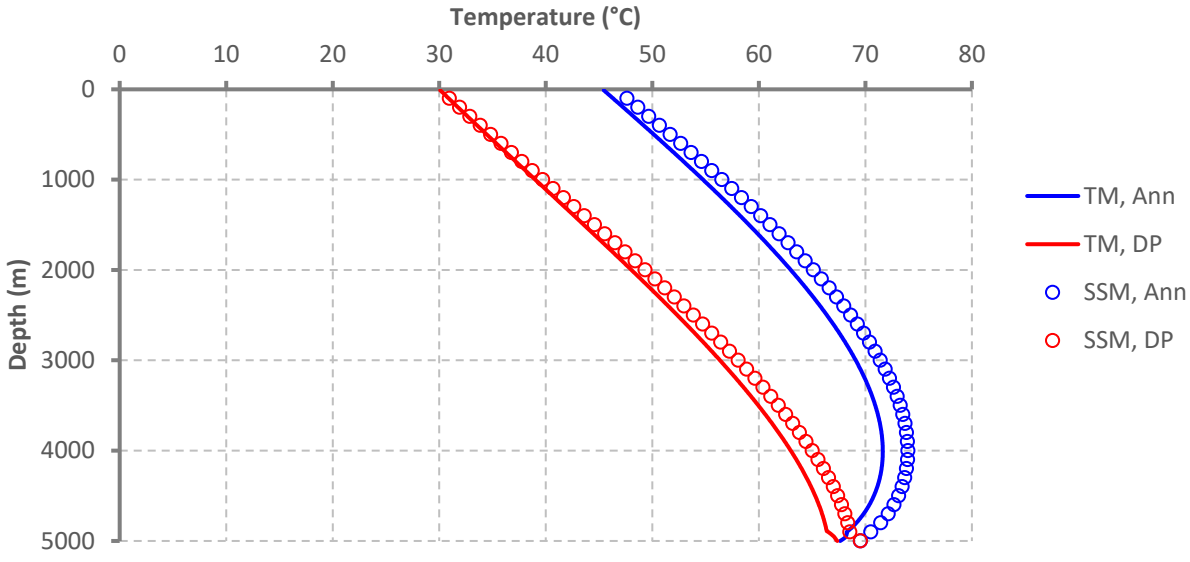

Figure 19: Wellbore temperature comparison between transient and steady state models (case 2). Geothermal gradient omitted to improve horizontal axis resolution.

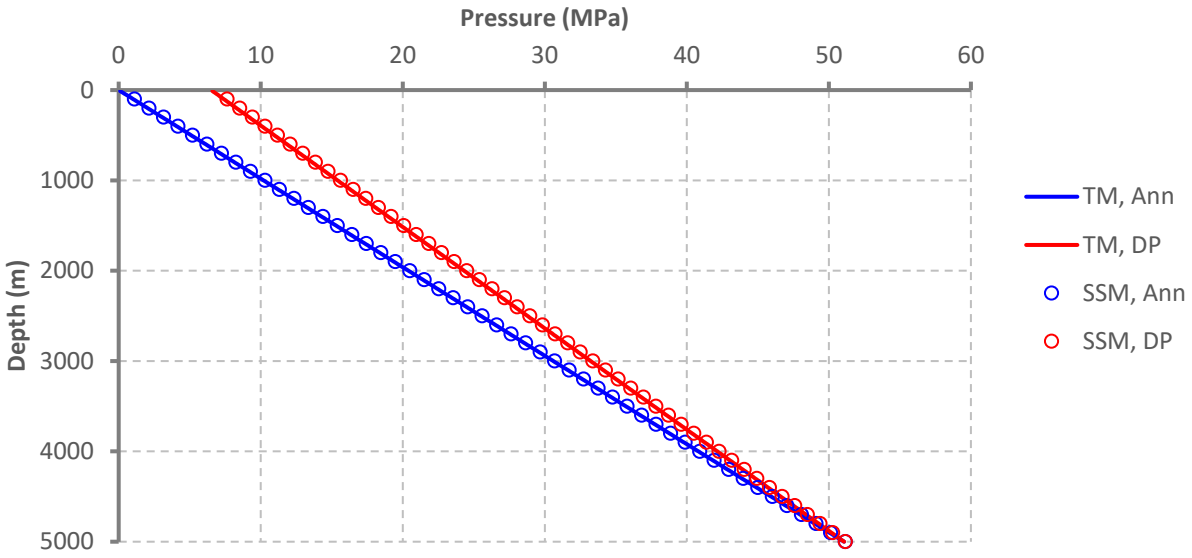

Figure 20: Wellbore pressure solution comparison between transient and steady-state models (case 2)

Since the form of the momentum/pressure equations are similar between the transient and steady-state models, their pressure solutions are nearly identical. The steady-state model predicts on average 1.1% higher wellbore pressures than the transient model.

However, the differences in the temperature solutions between the two models is greater. The tables below summarize the percent difference in the temperature and pressure solutions.

Table 8: Percent difference between the steady-state and transient model temperatures (calculated as SSM relative to TDM)

	Case 1: Carbon Steel (CS) String				**Case 2: Hypothetical IDP String**			
	Average	10th Percentile	50th Percentile	90th Percentile	Average	10th Percentile	50th Percentile	90th Percentile
Entire Wellbore	6.0%	4.0%	6.6%	6.9%	2.9%	1.8%	3.2%	3.4%
Drill Pipe	5.9%	3.7%	6.6%	6.8%	2.5%	1.1%	2.9%	3.2%
Annulus	6.1%	4.4%	6.6%	6.9%	3.3%	3.1%	3.3%	3.4%

Table 9: Percent difference between the steady-state model and transient model pressures (calculated as SSM relative to TDM)

	Case 1: Carbon Steel (CS) String				**Case 2: Hypothetical IDP String**			
	Average	10th Percentile	50th Percentile	90th Percentile	Average	10th Percentile	50th Percentile	90th Percentile
Entire Wellbore	1.1%	-0.1%	0.4%	2.4%	1.1%	0.2%	0.5%	2.1%
Drill Pipe	1.0%	-0.1%	0.7%	2.6%	0.9%	0.2%	0.6%	2.1%
Annulus	1.2%	-0.1%	0.2%	2.0%	1.4%	0.2%	0.4%	2.0%

3.6 Modelling Transient Operations

3.6.1 Connections (No Circulation)

When making a connection while drilling, the following actions are taken:

1. Circulation is ceased ("pumps-off")
2. Joints are made-up and connected to the top of the string
3. Circulation initiated
4. Drilling continues (drill string gradually lowers)

While circulating, the fluid keeps the bottom-hole fluid temperatures relatively low. Once circulation stops, the stagnant fluid in the wellbore begins to heat up gradually from the surrounding rock. It is feasible that during pumps-off, the wellbore fluid heats up beyond the temperature limits of the BHA components.

The transient model can help evaluate the maximum connection times at various depths in the well at which the temperature limits of key components are not exceeded.

Using the case 2 transient model from the previous section, we can model a connection being made at a depth of 5 km:

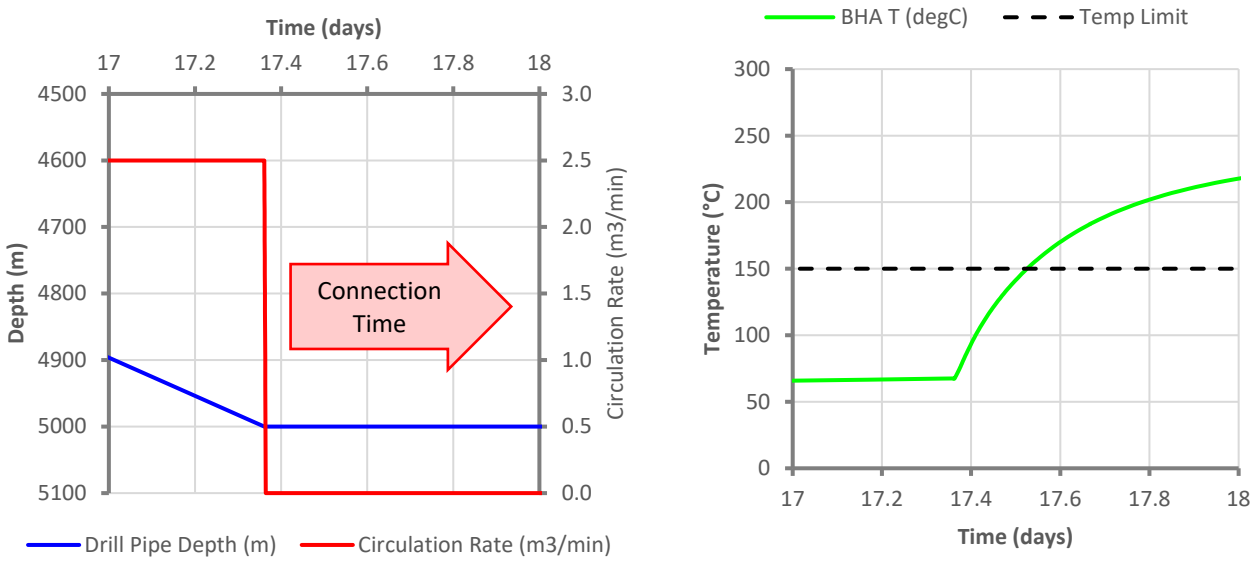

Figure 21: Connection transient model results

During pumps-off, while the connection is being made, the stagnant fluid at the bottom of the well begins to heat up dramatically due to the high rock temperatures at these depths (virgin rock temperature = 260 °C).

The time it takes the bottom-hole fluid to reach the 150 °C temperature limit is about 233 minutes. With this hypothetical IDP, the rig has more than enough time to make connections before the temperature-sensitive components heat up beyond their limits. However, at deeper depths (i.e. hotter rock), and with less thermally resistive IDP, the time it takes to reach the 150 °C limit will decrease – potentially putting pressure on the rig to make connections fast enough to avoid excessive wellbore heating during pumps-off.

3.6.2 Formation Kicks

In addition to modelling standard drilling operations, the model is also capable of modelling fluid kicks from the formation. While drilling, the circulating fluid will keep the wellbore and the BHA components cool. However, in the case of hot fluid ingress from the surrounding rock formation, there may be a risk that the circulating fluid is not enough to dilute the hot kick fluids to

- maintain the wellbore below the temperature limit, or
- prevent flashing of return fluids at surface

The transient model can be used to explore the impact of kicks on the fluid temperatures in the well, as well as return temperatures at surface. Again, using the case 2 transient model, we can model taking a kick at 5 km deep:

Table 10: Case 2 transient model + kick model inputs

Model Input	Units	Value
Kick Fluid	-	Water
Kick Volume	bbl	10
Kick Rate	m3/min	1.0
Kick Duration	min	1.6
Kick fluid temperature	°C	260 (rock temperature)

The figure below shows the annular fluid temperature profile during and after the kick:

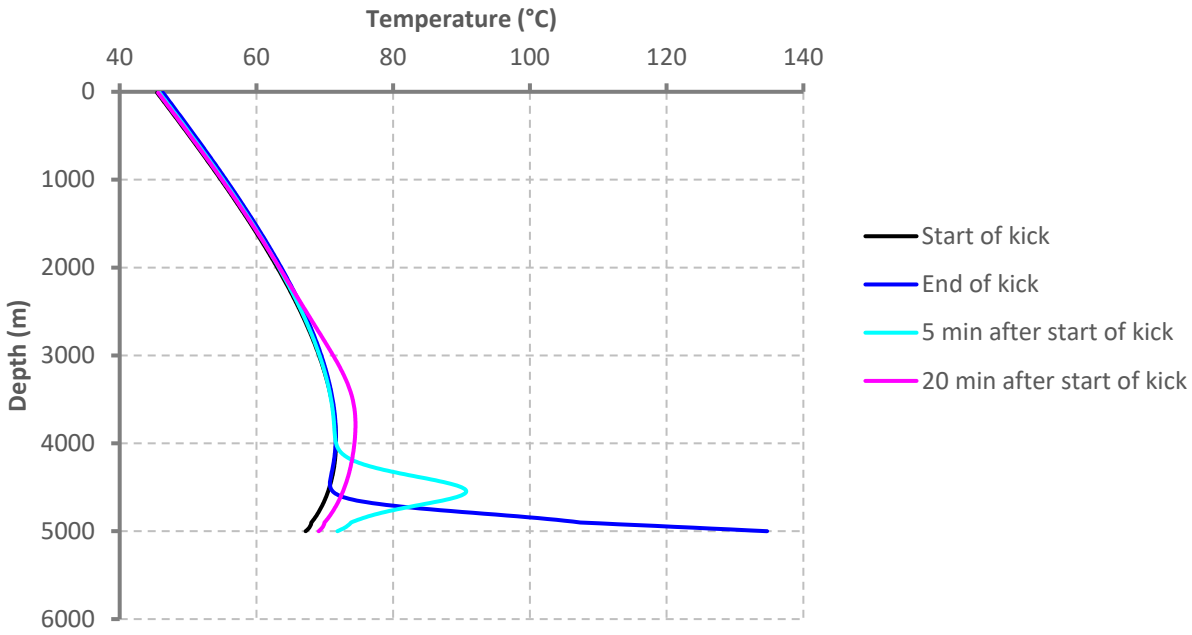

Figure 22: Modelled results of formation kick on annular temperature profile

During the kick, bottomhole temperatures climb quickly due to entry of hot kick fluids into the wellbore but is quickly diluted by the cold drilling fluid leaving the bottom of the drill string. As the slug of hot fluids moves upwards in the annulus, the temperature cools as it continues to be diluted with cold circulating drill fluids and heat exchange with the drill pipe fluids. By the time the slug reaches the top of the annulus, the excess heat has largely left the annular fluid, and the outlet temperatures are relatively unaffected.

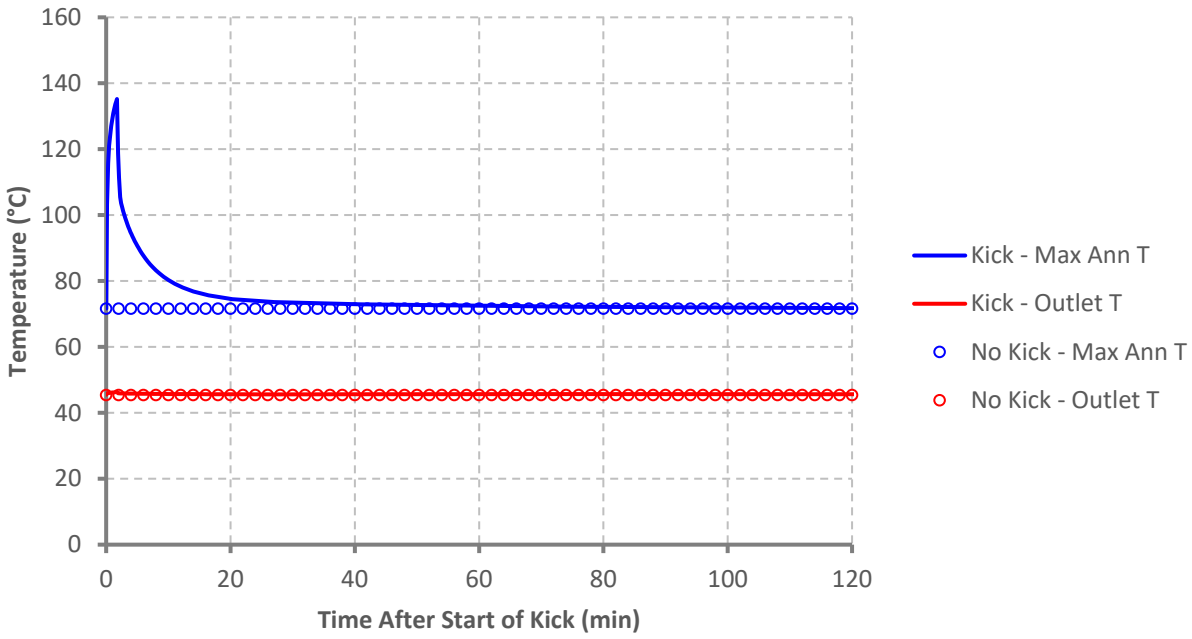

Figure 23: Max downhole circulating, and return temperatures during a kick

Due to the finite-difference approach to modelling, the authors recognize the impact of numerical dispersion on the simulation of the "slug" flow of hot kick fluids up the annulus (similar to the numerical dispersion often seen in reservoir modelling of immiscible flood fronts). Reducing the axial grid block size would reduce the impact of numerical dispersion on the simulation results.

Regardless, the kick functionality of the transient model can be used to sensitize the impacts of kick size and influx rate on fluid temperatures. The follow-on effects on temperature sensitive components in the BHA and drill string, as well as the return temperatures, can be evaluated.

3.6.3 Running-in-hole (RIH)

As mentioned, and illustrated above, fluid circulation minimizes the fluid temperatures within the wellbore. However, during periods of no-flow, the wellbore fluids quickly start to equilibrate with virgin rock temperatures.

When swapping drill bits, the drill string is tripped out of and back into the hole. During these operations while the rig is not circulating, the wellbore fluid temperature will begin to increase. As the BHA is lowered back into the hole, there is a risk that it may encounter fluid temperatures greater than the limits of the sensitive components. The transient model can be used to model the heating of the stagnant wellbore fluids, and subsequently the temperatures observed by the BHA while tripping back in.

Using the case 2 transient model, we can model a bit change at 5 km deep:

Table 11: Case 2 transient model + bit change parameters

Model Input	Units	Value
Tripping out of hole speed	ft/hr	1,500
Tripping in hole speed	ft/hr	1,000
Time to change bit	min	240

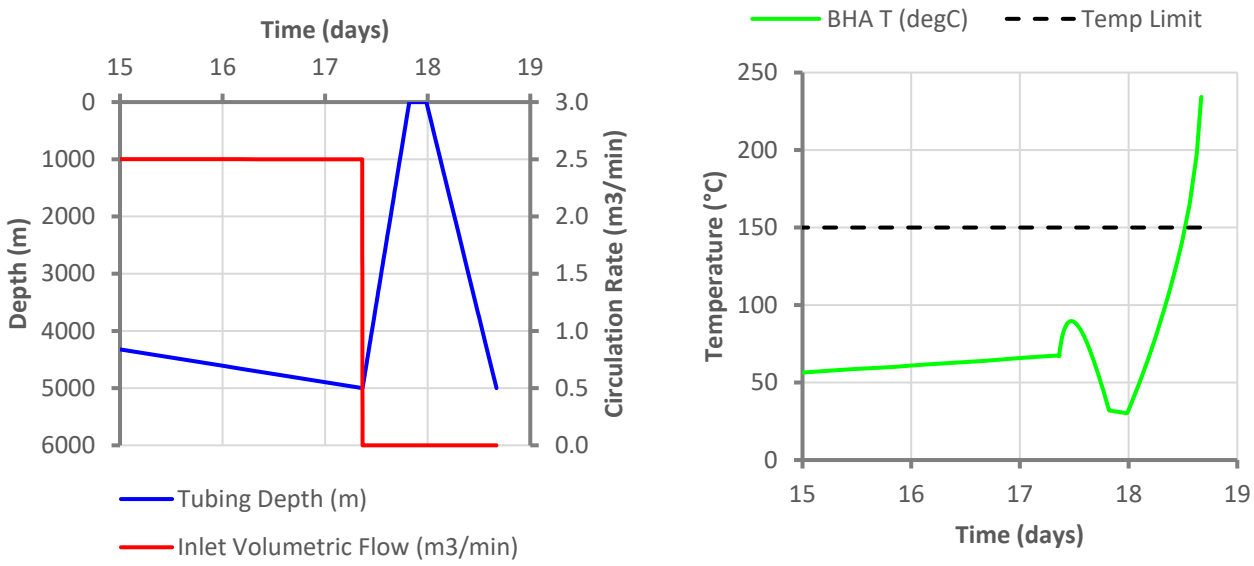

Figure 24: Running-in-hole transient model results

Although the insulated drill pipe keeps the circulating temperatures much below the 150 °C temperature limit, once circulation ceases, the temperatures quickly equilibrate with the virgin rock temperature. While running in hole, the temperatures observed at the BHA far exceed the tolerable temperatures.

To prevent the BHA from experiencing temperatures >150 °C, periods of circulation can be introduced to the tripping in hole procedure (a.k.a "washing-in") to gradually cool the wellbore fluids while descending. The refinement of tripping in procedures can be guided by simulation results produced by the transient model.

3.7 Field Validation of Transient Model

3.7.1 Eavor-Deep™ Overview

The Eavor-Deep™ project utilized Eavor's proprietary drilling technology – including an insulated drill pipe – to drill a single well, with sidetrack, > 5km deep in granite with rock temperatures of ~250°C. The well was constructed in New Mexico, USA where local geothermal gradients can exceed 50 °C/km. The insulated drill pipe technology developed by Eavor is a 5.5" base pipe with several insulating layers that can handle very high torque and tensile loads, and enable drilling techniques at depths 7 km or greater.

The purpose of the Eavor-Deep™ Project was to demonstrate all the technical elements required to construct commercial Eavor-Loops™ in deep, high temperature hard rock. The single well and sidetrack design was selected to replicate the first half of a commercial Eavor-Loop™ (i.e. the inlet or outlet well).

In addition to temperature measurements from Measurement While Drilling (MWD) tools, temperature sensors were located in various parts of the drill string to record annular fluid temperatures for the purposes of validating Eavor's transient thermodynamic drilling model.

3.7.2 Prediction of Eavor-Deep™ Drilling Temperatures

The transient model was used to predict the temperatures experienced while drilling Eavor-Deep™. The model was history matched using 3 bit runs worth of data spanning ~4 days, comprised of

- Return temperatures,
- MWD temperatures,
- Sensor temperatures, and
- Standpipe pressure

Inputs into the model consisted of

- Tubing depth,
- Hole depth,
- Circulation rate,
- Inlet fluid temperature, and
- Mud rheological parameters

History match parameters included:

- Drill pipe thermal resistance,
- Rock thermal conductivity, and
- Temperature gradient

The bounds on the history matching parameters were based on the range of expected pre-drill estimates for each. The history match was performed using a genetic algorithm to minimize an objective function specified as a weighted sum of squared errors between the model's prediction and the measured data.

Figure 23 below shows the measured and predicted sensor temperatures every 5 minutes. Over the displayed period, the sensor was located between 215-220 m above the bottom of the drill string. The period used for history matching the model and the model's forecast are denoted with the vertical line and accompanying annotations. The training and matching period was selected because of its relative high data quality, deep depths (between 4,100 and 5,100 m), and spanning portions of the well where estimated rock temperatures were in the range of 200 °C.

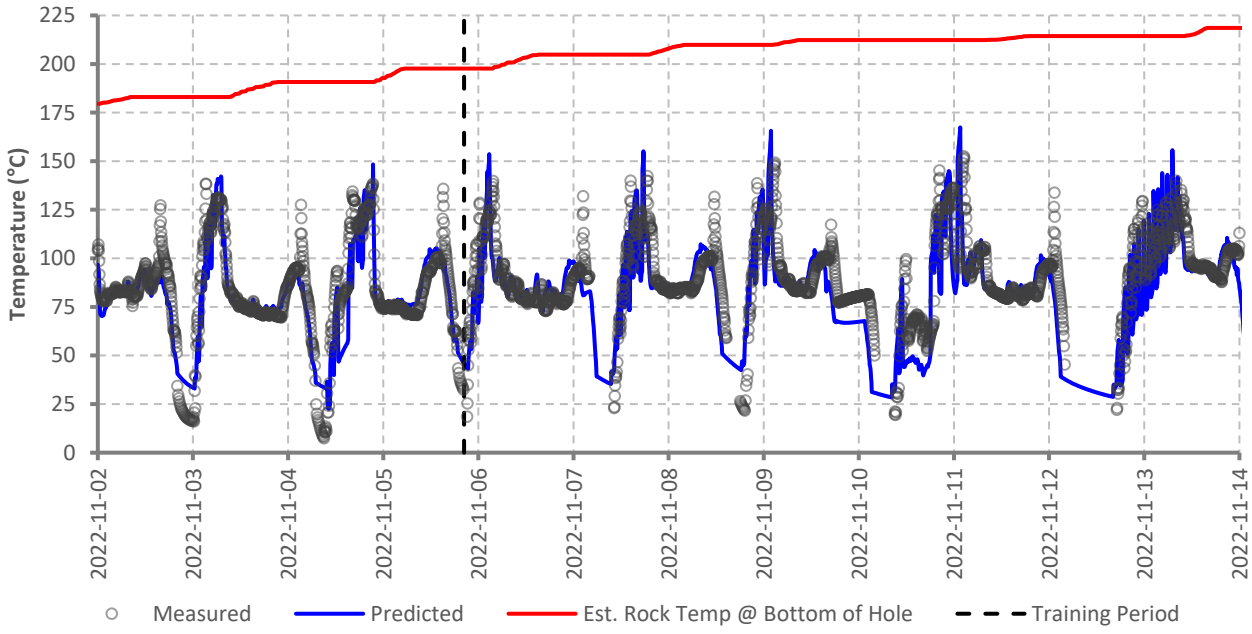

Figure 25: Eavor-Deep™ measured and predicted BHA sensor temperatures

Visually, the model does a good job of matching the transient temperature measurements over both the training and hold-out data. Circulating temperature error statistics are summarized in the histogram and Table 12 below.

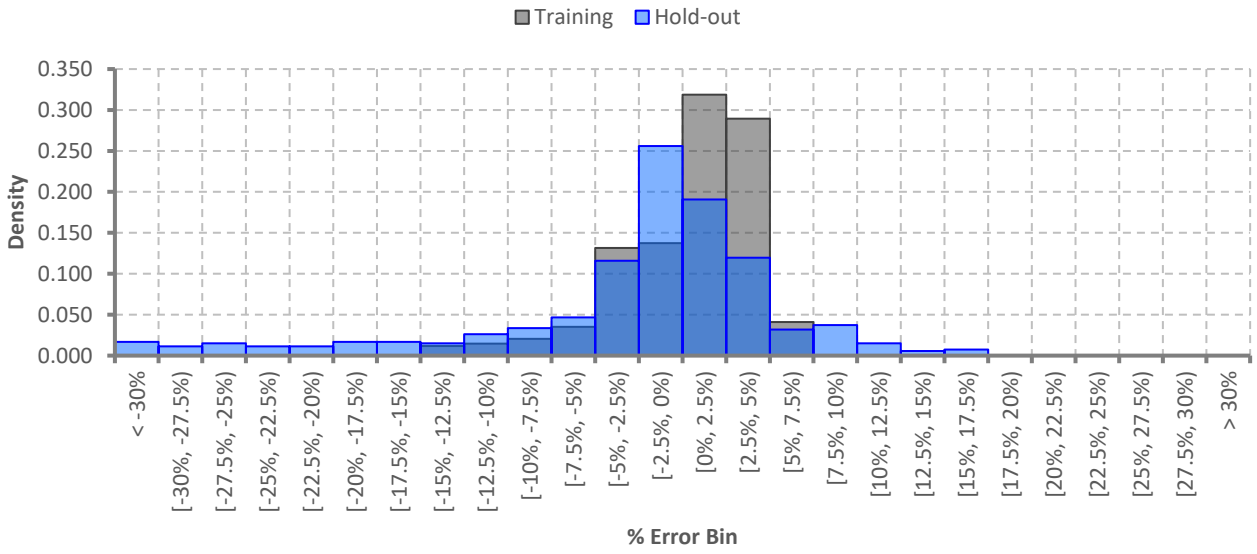

Figure 26: Histogram of circulating temperature model errors (at sensor)

Table 12: Transient model circulating temperature summary statistics for Eavor-Deep™

Period	10th Percentile Error	50th Percentile Error	90th Percentile Error	Between +/- 10% Error	Between +/- 15% Error
Training	-4.7%	1.2%	4.5%	97.4% of points	100% of points
Hold-out	-14.8%	-0.9%	4.9%	83.2% of points	89.3% of points

As expected, the match on the data between the training period is better than the hold-out period. However, the median (50th percentile) model error is in the 0% range for both periods.

The transient model provides accurate predictions of real circulating wellbore temperatures while drilling.

3.7.3 Theoretical IDP Cooling

As shown in Figure 25, the IDP used in the Eavor-Deep™ trial was able to maintain circulating temperatures below 150 °C at the bottom of the hole. The same history matched model was run with standard drill pipe thermal resistance numbers and re-simulated to show the theoretical cooling provided by the IDP technology .

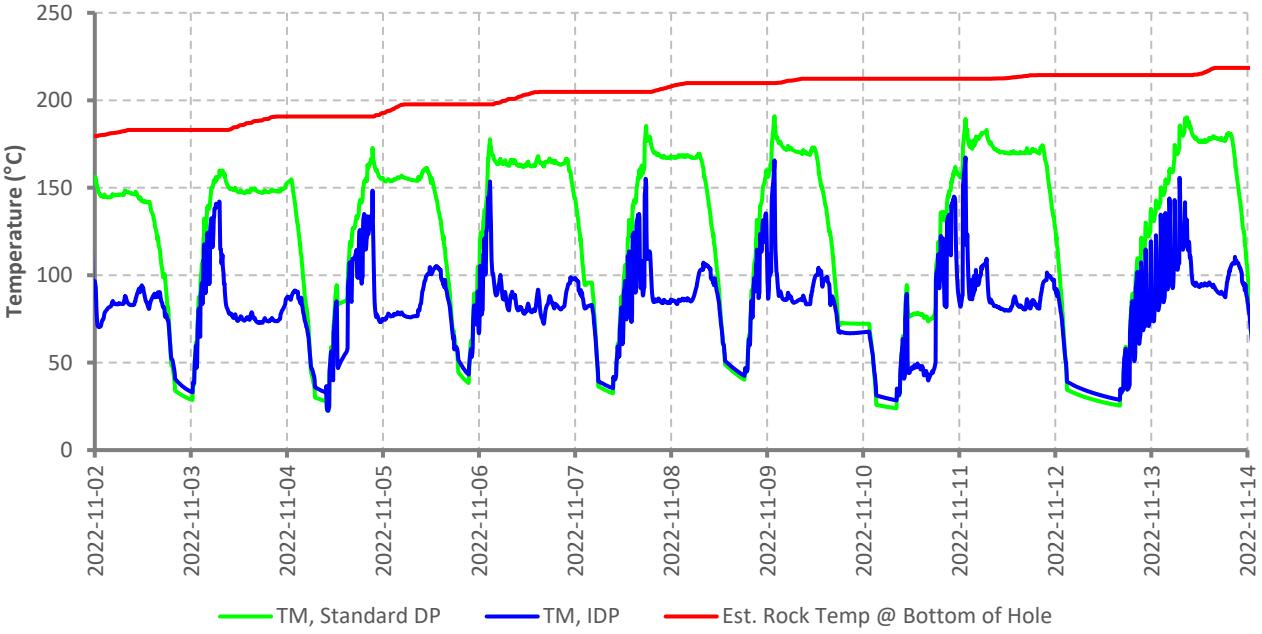

Figure 27: Simulated circulating temperatures for IDP and standard drill pipe

Over the simulated period, the IDP reduced downhole circulating temperatures by up to 90°C (with a median of 61°C). The model suggests that standard drill pipe would have been unable to maintain circulating temperatures below the 150°C tool limit and therefore drilling this well was possible only because of Eavor's IDP technology

In addition to proving out other drilling technologies, Eavor-Deep™ has proven that IDP unlocks hotter exploitable rock temperatures for MCLGS.

CONCLUSIONS

Eavor's proprietary MCLGS Eavor-Loop™ technology allows for the exploitation of geothermal energy around the globe. The levelized cost of energy (LCOE) is largely driven by rock temperatures – the hotter the rock, the better the economics of a MCLGS project. To date, directional drilling and magnetic ranging tools, which are critical to the development of MCLGS projects, have an upper temperature limit above which they are no longer functional.

To enable the drilling of HPHT wells for MCLGS, the developer needs to ensure cool wellbore fluid temperatures to prevent BHA component malfunction.

The steady-state and transient models presented above can predict operational temperatures in the wellbore, allowing for effective engineering design of HPHT well and drilling programs, as well as operational support during execution. The steady-state model can be used as an effective tool to quickly evaluate a range of scenarios, while the transient model can be used for detailed design.

As proven at Eavor-Deep™, drill pipe with increased thermal resistance (IDP) is a feasible method for maintaining cool downhole circulating temperatures, enabling the drilling of high-temperature hard rock formations for development of MCLGS projects.

REFERENCES

Beckers K F., and Johnston, Henry E.: Techno-Economic Performance of Eavor-Loop 2.0, Proceedings, 47th Workshop on Geothermal Reservoir Engineering, Standford, California (2022).

Beckers, K. F., Rangel-Jurado, N., Chandrasekar, H., Hawkins, A. J., Fulton, P. M., and Tester, J. W.: Techno-Economic Performance of Closed-Loop Geothermal Systems for Heat Production and Electricity Generation, Geothermics 100 (2022): 102318.

Ramey Jr, H.: Wellbore heat transmission, Journal of Petroleum Technology 14.04 (1962).

Toews, Matt, and Holmes, Michael: Eavor-Lite Performance Update and Extrapolation to Commercial Projects, GRC Transactions, Vol. 45 (2021).

National Institute of Standards and Technology. (2020). REFPROP

Beel, Ian H., and Wronksi, Jorrit, and Quoilin, Sylvain, and Lemor, Vincent.: Pure and Pseudo-pure Thermophysical Property Evaluation and the Open-Source Thermophysical Property Library CoolProp, Industrial & Engineering Chemistry Research 53, no. 6 (2014), 2498-2508.

Holmes, Michael, Toews, Matt, and Jenkins, Jesse, and Sepulveda, Nestor: Multilateral Closed-Loop Geothermal Systems as a Zero-Emission Load-Following Resource, GRC Transactions, Vol. 45 (2021).

Hasan, A.R., Kabir, C.S.: Fluid Flow and Heat Transfer in Wellbores 2nd Edition (2020), Society of Petroleum Engineers.

Finger, John, and Jacobson, Ron, and Whitlow, Gary, and Champness, Tom: Insulated Drill Pipe for High-Temperature Drilling (2000), Sandia National Laboratories.

Oldenburg, C., Pan, L., Muir, M., Eastman, A., and Higgins, B.S.: Numerical simulation of critical factors controlling heat extraction from geothermal systems using a closed-loop heat exchange method, Proceedings, 41st Workshop on Geothermal Reservoir Engineering, Stanford, California (2016).

Horne, R.: Design considerations of a down-hole coaxial geothermal heat exchanger, Geothermal Resources Council Transactions (1980)

Jang, M., and Chun, T.S., and An, J.: The Transient Thermal Disturbance in Surrounding Formation during Drilling Circulation. Energies (2022), 15, 8052. https://doi.org/10.3390/en15218052

Hasan, A. R., and Kabir, C. S.: Aspects of Wellbore Heat Transfer During Two-Phase Flow, SPE Prod & Fac 9 (1994): 211–216. https://doi.org/10.2118/22948-PA

Kabir, C. S., Hasan, A. R., Kouba, G. E., and M. M. Ameen: Determining Circulating Fluid Temperature in Drilling, Workover, and Well Control Operations, SPE Drill & Compl 1 (1996): 74-79. https://doi.org/10.2118/24581-PA

Hasan, A. R., and Kabir, C. S.: Wellbore heat-transfer modeling and applications, Journal of Petroleum Science and Engineering, Volumes 86-87, (2012): 127-136. https://doi.org/10.1016/j.petrol.2012.03.021